Electricity Generation from Paper Vibration by Electrostatic Induction

January 2016

Evi OKTAVIA

Electricity Generation from Paper Vibration by Electrostatic Induction

A Dissertation Submitted to

The Graduate School of Life and Environmental Sciences,

The University of Tsukuba

in Partial Fulfillment of the Requirements

for the Degree of Doctor of Philosophy in Bioresources Engineering

(Doctoral program in Appropriate Technology and Sciences for Sustainable Development)

Evi OKTAVIA

TABLE OF CONTENTS

LIST OF FIGURES

LIST OF TABLES

LIST OF ABBREVIATION

AC	Alternating Current
DC	Direct Current
HBKP	Hardwood Bleached Kraft Pulp
LED	Light emitting diode
MEMS	Micro Electro Mechanical Systems
FFT	Fast Fourier Transform
PFI mill	Paper and Fiber Research Institute mill
PTFE	Polytetrafluoroethylene or Teflon
PVDF	Polyvinylidene fluoride
PZT	Lead zirconate titanate
SBKP	Softwood Bleached Kraft Pulp
TriboEG	Triboelectric generator
VEH	Vibration Energy Harvesting
Hz	Hertz
µA	Micro Ampere
mC/m^2	Micro Coulomb / meter square
mV	Milli Volt

MΩ	Mega Ohm
nW	Nano Watt
rpm	Rotation per minute
C	Capacitance
F	Farad
f	Frequency
P	Power
PF	Power factor
Q	Reactive power
R	Load resistance
S	Apparent power
T	Period time
X	Reactance
Z	Impedance
ω	Angular frequency
θ	Impedance angle

CHAPTER I

1 INTRODUCTION OF THIS RESEARCH

Nowadays, ICT (information and communication technology) devices such as smartphones, wearable devices, and wireless sensors are developing to implement new societies where IoT (internet of things) and IoE (internet of everything) are ubiquitous. Those devices and tools always or frequently on demand access to internet and therefore require electric power sources. In place of conventional power sources such as battery that must be frequently replaced and disposed, new fabrication technologies have recently resulted in micro fuel cells (Paradiso & Statner, 2005) or exploitation of renewable energy resources in the device's environment (Khoury, Tourtoller, & Schroder, 1999). Energy harvesting also referred to as energy scavenging has a large variety of energy sources and conversion methods. The energy sources for energy harvesting are ambient and not autonomous, for example, light (direct sunlight, ambient light and artificial light), heat (temperature variation and thermoelectric), vibration (mechanical and piezoelectric), waves (acoustic noise and ambient radio frequency), static electricity, and human life (walking step, body heat, and blood flow) (Bhatnagar & Owende, 2015).

In the past decades, energy harvesting has attracted global attention. Emerging new technology such nanogenerator can harvest energy from waste source i.e. vibration, heat, and light. A non-traditional way e.g. microelectromechanical system (MEMS) devices are capable to operate at low power. Several attempts have been made to harvest energy from mechanical movements in ambient environments which are known as "waste" sources. Figure. 1.1 shows available power in ambient environment.

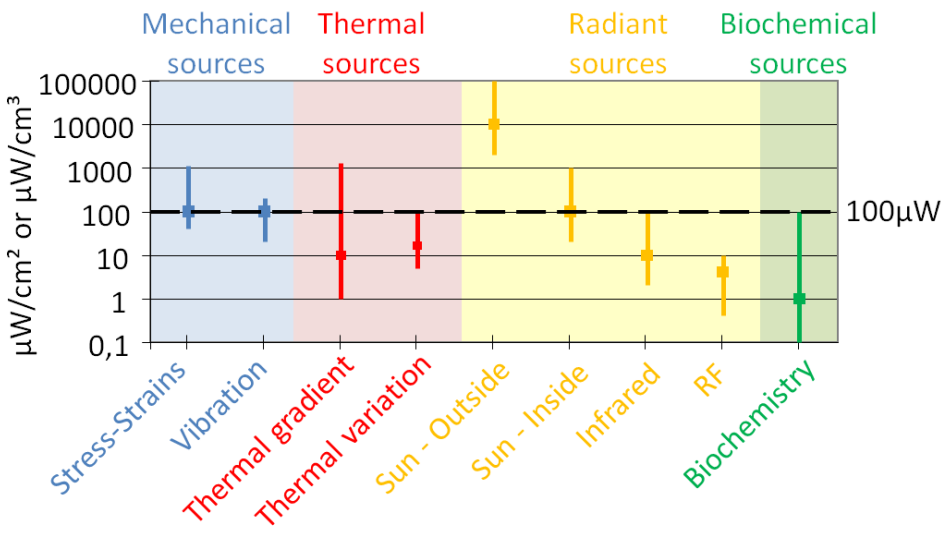

Figure 1Ambient sources power density (Boisseau, Despesse, & Seddik, Electrostatic conversion for vibration energy harvesting, 2012)

Mechanical sources even tough do not provide high power density but quite enough to light some LED lamps in terms of the vibration energy harvesting (VEH) application. In the early experiment, reported the generation of power was reported about 0.3 μW using magnetic converter from an ambient environment (Shearwood & Yates, 1997) and the theoretical energy induction of the nonlinear microsystem model were calculated (William & Yates, 1996).

In VEH, converters play important roles. Other types of converter or generator such as piezoelectric (Briscoe, et al., 2013), and electromagnetic (Shearwood & Yates, 1997) inductions have drawn many interests of researchers. Advantages and disadvantages of each technique could be criteria to choose the suitable applications as mentioned in Table 1.1 (Wang & Yuan, 2007).

Table 1.1 Induction technique comparison

Type	Advantages	Disadvantages
Electromagnetic	no smart material needing	Bulky size magnets and pick-up coil
	no external voltage source	Difficult to integrate with MEMS
		max 0.1 V voltage generation
Electrostatic	no smart material needing	Needed charge or external source
	MEMS compatibility	Needed some mechanical constrains
	Voltages generation 2-10V	Parasitic capacitive
Piezoelectric	no external source needed	Depolarization
	Voltages generation 2-10V	PZT brittleness
	Compactable configuration	Poor coupling in PVDF-piezo
	MEMS compatibility	Charge leakage
		High output impedance

Demands for eco-friendly electronics are also increasing. Paper, formed as a cellulosic fibers network, has been recognized as an eco-friendly and sustainable material. It has some advantages such as light weight, flexibility, and low cost. Paper, due to hydroxyl groups of cellulosic fibers, tends to have negative charge in spite of neutral surfaces. Thus electrostatic induction is suitable for VEH.

Paper as a dielectric material seems suitable to apply in (William & Yates, 1996) electrostatic induction type. Paper also have to fulfill the concept of electrostatic vibration energy harvesting system: 1) has two electrodes called "guard and collector" electrodes, or "moving and static" electrodes, or "dynamic and static" electrodes, etc. that has potential differences to obtain charge movement, 2) has a generator called "electret", (formed of *electr-* from "electricity and *-et* from "magnet") is a dielectric material that has a quasi-permanent electric charge or dipole polarization. Mostly made from polymer (PTFE or CYTOP), 3) has a proof or mobile mass, mostly made from SiO_2 or Si_3N_4, and 4) has a spring system to generate a resonance phenomenon (Takahashi, Suzuki, Nishida, Yoshikawa, & Aoyagi, 2012).

Electret as a dielectric material should be treated first in order to deposit a charge onto its surface. Other tools, such as soft X-ray (Honzumi, Ueno, Hagiwara, & Suzuki, 2010), ionic hair dryer (Saad, Mescheder, Muller, & Nimo, 2010), and even manual rubbing with opposite materials (Karagozler, Poupyrev, Fedder, & Suzuki, 2013), also can be applied. The most useful tool for electret charging is the corona treatment (Paajanen, Wegener, & Gerhard-Multhaupt, 2001).

Triboelectric effect can be achieved by electret charging. The semi-permanent negative charge of electret accumulates on its surface due to high voltage charging using corona treatment with two different materials with a high affinity difference. Table 1.2 shows the list of triboelectric materials (Alphalab Inc., 2012). PTFE has a lower electron affinity than paper, thus PTFE charge is highly negative and can act as an electric field source. The charges on a PTFE film

near an electrode can attract free charges of the electrode or any conductive materials. A relative movement of an electret layered on paper as a fixed part to the moving part that vibrates due to vibration, sound, or noise as mechanical source provides an electric potential difference between the electrodes or further converts it into electrical energy. In this research, paper can act as a supporting material with stiffness and also elasticity in propagating vibration. In terms of the triboelectric effect, paper is also a rigid and weak polyelectrolyte due to its process in papermaking (Hagiopol & Johnston, 2011). The trapped moisture and additives in paper sheet can bridge embedded PTFE electret and conducting electrodes.

Table 1.2 Triboelectric series

Materials	Affinity (nC/J)
Polyurethane foam	+ 60
Nylon	+ 30
Paper (uncoated)	+10
Cotton	+ 5
Wool	0
Epoxy (circuit board)	-32
Polyimide	-70
Cellulose nitrate	-93
PTFE	-190

1.1 Objective

This thesis aims to clarify the relationship between the vibration damping and mechanical properties of paper to realize efficient power generation, and to create a triboelectric power generator to convert this sonic vibration energy into electrical energy to power microelectronics embedded on paper.

1.2 Research scheme

The overall research schematic of VEH is presented in Figure. 1.2. This research focusing on the paper propagating vibration as a model of sound in environmental sources and its role in electrostatic converter or induction, and later the circuit set-up using capacitor as storage system in simple electronic device. Storage systems including capacitors and electronic devices as end products may vary from wireless sensor, MEMS, or low power interactive multimedia.

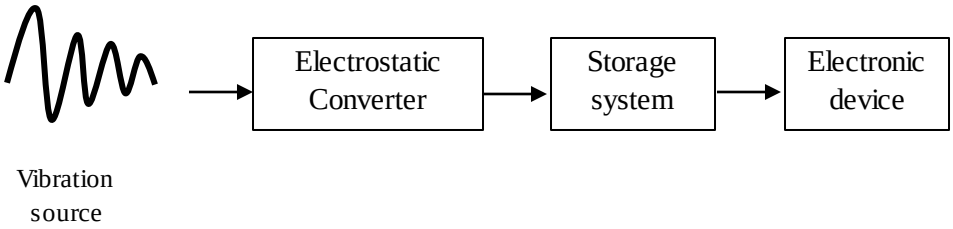

Figure 2 Schematic of vibration energy harvesting

This dissertation consisted of 5 chapters and an appendix related to research scheme in Figure 1.2. Chapter II discusses the sound levels development of various types of paper propagating sonic waves and relationship of beating degree of paper and its elasticity in sound propagation. Chapter III discusses resonance behavior of out-of plane paper vibration. Chapter IV provides generated voltage of in-plane paper vibration. Chapter V provides the overall conclusion. The power determination of paper-based generator circuits is provided in Appendix.

CHAPTER II

2 SOUND LEVELS DEVELOPMENT OF VARIOUS TYPES OF PAPER PROPAGATING SONIC WAVES

2.1 Introduction

Paper has high elastic moduli although it consists of flexible, lightweight, and hygroscopic plant fibers. Paper, formed as a cellulosic fiber network, has been recognized as an eco-friendly and sustainable material with advantages such as light weight, flexibility, recyclable and low cost. Among those, high rigidity for light weight is particularly attractive for VEH because acoustic waves tend to propagate fast. One of the material parameters to determine vibration energy damping is Young's modulus that achieves the highest value in the direction of fiber alignment called the machine direction (MD) for machine-made paper and with the sheet with the highest stress applied during drying (Haberger, Mann, & Baum, 1979). Therefore, the directionality is also a parameter in the case of paper vibration properties. Ultrasonic waves propagating through paper are classified into plate waves has been investigated (Lamb, 1910). Plate waves have a number of nodes and differ from bulk waves in this respect. The propagation velocity of plate waves depends on the frequency; therefore, the plate wave is called "dispersive" (Khoury, Tourtoller, & Schroder, 1999). In addition, the velocity depends on the density and thickness of the paper. The dispersion equation of plate waves was derived for paper (Haberger, Mann, & Baum, 1979). Although mechanical vibration sources do not provide high power density, but provide much enough power to turn on LEDs and operate low-power-consumption devices by means of the vibration energy harvesting (VEH) applications. In addition, posters put up in halls

could be interactive once installed with a power generator that is responsive to human voice and an actuator in series on it.

In VEH, other types of converter or generator based on principles such as piezoelectric, electromagnetic (Shearwood & Yates, 1997), magnetostrictive (Wang & Yuan, 2007) and electrostatic (Boisseau, Despesse, & Seddik, Electrostatic conversion for vibration energy harvesting, 2012) (William & Yates, 1996) inductions have drawn many interests of researchers. The principle of electrostatic induction applied in this work is defined as the redistribution of electric charge on one material under the influence of nearby objects called "electret" that has a permanent electric charge.

This chapter aims to transfer the energy held in paper as vibrations from environmental noise, sound, and voice with as less loss as possible with developing the self-powered paper devices using electrostatic generators. Storage systems including secondary cells and capacitors might be applied, but kept to minimum for lightness and short-time use. Continuous environmental noises from road traffic, production factories, and construction sites and so on are the target vibration sources. A simple measurement method of the vibration power is to detect a sound, that is, one of the converted forms of vibration using condenser microphone principle.

The purpose of the research in this chapter is to clarify the relationship between the vibration damping and mechanical properties of paper. The vibration damping was evaluated by measuring the sound power level of the constant sound source through a sheet of various kinds of commercially-available paper. Subsequently, to avoid the influence of constituent materials such as fibers and additives, and papermaking conditions, laboratory sheets were prepared from bleached kraft pulps. These samples were subjected to the concurrent measurement of the sound power level and Young's modulus of the identical sheets.

2.2 Experimental

2.2.1 Structural properties of samples

Several types of commercially available paper samples were tested and their physical properties are listed in Table 2.1. The thickness of the paper was measured using a micrometer (TW-21, Tozai Seiki, Japan) according to ISO 534. The apparent bulk density was calculated by dividing the measured grammage by the total thickness. For laboratory sheets prepared from hardwood bleached kraft pulp (HBKP), the density was considered as apparent sheet density. Hereafter, both densities are referred to only "density".

Table 2.1 Structural properties of commercially-available paper samples

Key	Type of paper	Grammage (g/m^2)	Thickness (μm)	Density (kg/m^3)
A	Food wrapping paper	14	19	739
B	Wax paper	27	27	991
C	Towel paper (Kimtowels, Kimberly-Clark)	19	60	311
D	Copy paper (Mitsubishi Paper)	69	90	766
E	Envelope paper	76	97	782
F	Condenser paper (OFS100P, Tomoegawa Paper)	90	103	872
G	Tracing paper	64	63	1015
H	Original nonwoven cloth	38	132	289
I	Silicone-coated glassine paper (Konos Papier, GmbH)	40	48	833

2.2.2 Laboratory sheets from pulps with different beating degrees

Laboratory sheets prepared from HBKP and softwood bleached kraft pulp (SBKP) with high beating degrees were tested. The pulps were soaked in deionized water for 12 hours, defibrated in a disintegrator for 5 minutes, and then beaten in a PFI mill to 5000, 10000 and 20000 revolutions (rev.). In addition to an unbeaten pulps were also used. The laboratory sheets were formed, pressed and dried according to ISO 5269-1 to reach the target grammages of 60, 80, 100, and 120 g/m^2.

Table 2.2 Structural properties of laboratory sheet samples

Beating degree (rev.)	HBKP			SBKP		
	Grammage (g/m^2)	Thickness (μm)	Density (kg/m^3)	Grammage (g/m^2)	Thickness (μm)	Density (kg/m^3)
Unbeaten	50	85	560	57	114	522
	83	139	553	79	153	546
	93	150	597	92	190	511
	110	181	589	117	221	509
5000	56	74	761	66	86	763
	77	102	740	70	93	745
	95	125	717	95	114	811
	105	137	756	116	145	819
10000	60	69	777	57	70	805
	81	101	758	78	92	834
	87	107	773	98	114	810
	110	132	785	114	132	860
20000	56	66	786	55	63	882
	83	94	805	74	80	848
	103	117	817	94	101	908
	115	132	823	114	121	983

2.2.3 Young's modulus of paper samples

Young's modulus is closely related to vibration or sound propagation in paper. Vibration energy cannot be completely maintained during its propagation in materials and it dissipates as heat by internal friction. Vibration damping is often represented by the damping ratio ζ, which describes how rapidly the oscillation decays from one bounce to the next, for example, in a system of a mass suspended from a spring, for example.

The resonance of a beam with a rectangular cross section leads to Young's modulus E as described by Eq. (1):

$$E=48\pi 2l4\rho fn2+18\Delta fn2\lambda n4T2 \qquad 1,$$

where T is the thickness of a beam sample, ρ is the density, l is the length, f_n is the nth natural resonance frequency, Δf_n is the nth full width at half maximum of the peak, and λ_n is the nth wavelength. Eq. (1) is transformed by applying the formula $\zeta = {}^{\Delta f_n}/_{2f_n}$ to Eq. (1)':

$$\zeta^2 = \frac{\lambda_n^4 T^2}{24\pi^2 l^4 f_n^2}\frac{E}{\rho} - 2 \qquad (1)',$$

Eq. (1)' indicates that the energy damping ratio squared ζ^2 is determined by specific Young's modulus E/ρ of paper in relation to the material's property if the sample dimensions are assumed to be constant.

Young's modulus E was determined from the ultrasonic velocity, which was measured using an ultrasonic tester (Sonic Sheet Tester-110, Nomura Shoji, Japan). This calculation is based on Eq. (2):

$$E_L = {V_L}^2\rho(1 - v_{12}v_{21}) \quad (2),$$

where E_L = Young's modulus in the machine direction (MD), V_L= the longitudinal velocity in MD, ρ=the density, v_{12} and v_{21} =two Poisson's ratios in the 1-2 plane. Paper is usually described as an orthotropic elastic material. MD is defined as the 1 direction and the cross direction as the 2 direction. For paper, the product of Poisson's ratios is typically as small as approximately 0.07 (Baum, Brennan, & Haberger, 1981). Therefore, Eq. (3) applies after rewriting E_L as E.

$$E = V_L{}^2 \rho \qquad (3)$$

V_L was measured in both MD and CD. The geometrical mean was adopted to calculate the E value.

2.2.4 Measurement of sound power level via paper vibration

Figure 2.1 shows a schematic representation of (a) the receiving unit used in this work for the sound level measurement and (b) a typical electret microphone.

An electret condenser microphone installed in a sound level meter (SL-1370, Custom Corporation, Japan) was implemented to receive acoustic waves and measure the sound level, or more accurately, the sound power level L_w as defined (Schlecther, 2006) in Eq. (4):

$$L_w = 10log_{10}\left(\frac{P}{P_0}\right)\text{dB} \qquad (4),$$

where P is the sound power and P_0 is the reference sound power equal to 10^{-12} W. The decibel (dB) is a logarithmic unit that expresses the ratio of two values of a physical quantity, often power or intensity. A 10 dB change is equal to a change in power by a factor of 10.

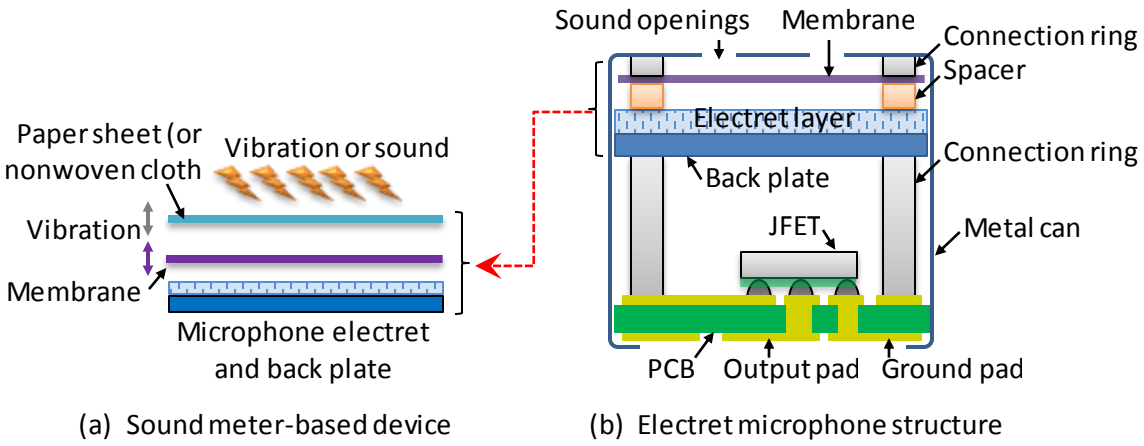

Figure 3 Schematic representation of (a) sound meter-based device for measuring sound level in this work and (b) typical electret

Condenser microphones are very popular for downsizability. They are equipped with a membrane functioning as a diaphragm or vibration plate that periodically change the relative position of electret to an electrode and transfers the vibration or sound to another form of signal, thus allowing a current to flow. Diaphragms are usually fabricated from plastic films with vapor-deposited metal or metal thin films. However, in this study, the vibration energy was evaluated using an electret microphone condenser with nonwoven cloth for protection from dust and airflow noise. The various types of paper were tested as substitutes of the nonwoven cloth to evaluate the rule of paper's type in vibration energy transfer.

Electrets of microphone condensers are dielectric materials with a permanent electric field that is achieved by a high voltage polarization process to order molecular dipoles permanently. An electret can be used effectively in cooperation with micromachining technology for small-scale fabrication and self-powered devices (Hsu, Hsich, Tai, & Furatani, 1996). There is another type of condenser developed more recently that is capable of ultrasound by detecting acoustic waves. Thin membranes 0.1-2.0 μm thick or very small gaps 0.05-1.00 μm thick can be fabricated using silicon micromachining techniques and assembled in that type of condensers and consequently serve competitive efficiency and wide bandwidth with piezoelectric transducers (Ladabaum, Jin, Hyongsok, Atalar, & Khuri-Yakub, 1998) (Eccardt, Niederer, Scheiter, & Hierold, 1996).

Various types of paper listed in Table 2.1 were tested as a substitute of the nonwoven cloth to evaluate the efficiency of vibration energy transfer. A small test piece of approximately 10 mm in diameter was cut out of each paper sample and mounted on the top of the receiving unit. As a standard sound source, a hair dryer (TID901, 1200 W, Tescom, Japan) in the cool mode was used, which was continuously operating for 2 min during the measurement. In measurement, the A-weighting mode was selected for frequency filtering and the protective cover, which consisted of a polymer foam sphere, was not attached. The distance between the microphone electret and the test piece of paper was approximately 0.01 mm. The background noise was 36.5±0.5 dB.

For the laboratory sheet samples, the ultrasonic propagation velocity and sound power level were measured simultaneously, as shown in Figure 2.2. The transmitted ultrasonic waves were partially converted to an audible sound that was detected by the sound meter.

Figure 4 Concurrent measurement of ultrasonic velocity and sound power level

2.3 Result and Discussion

2.3.1 Sound power level of commercially-available paper samples

Sound power is energy per unit area and thus proportional to amplitude squared of acoustic waves. In damped oscillation, the vibration energy is related to the damping ratio squared ζ^2 because ζ is proportional to the logarithmic amplitude decreasing ratio per cycle. Eq. (1)' describes that ζ^2 is proportional to the specific Young's modulus for the resonating beams with the same dimension, suggesting that there is a certain relationship between the sound power level and specific Young's modulus. Figure 2.3 shows the relationship between two physical values for various types of commercially-available paper. Symbols E, D, G, F, and I are consistent with those listed in Table 2.1. For the other samples, ultrasonic velocity and resulting Young's modulus could not be determined due to too small area or too soft structure causing strong acoustic attenuation. Unexpectedly, no systematic relationship was obtained between them.

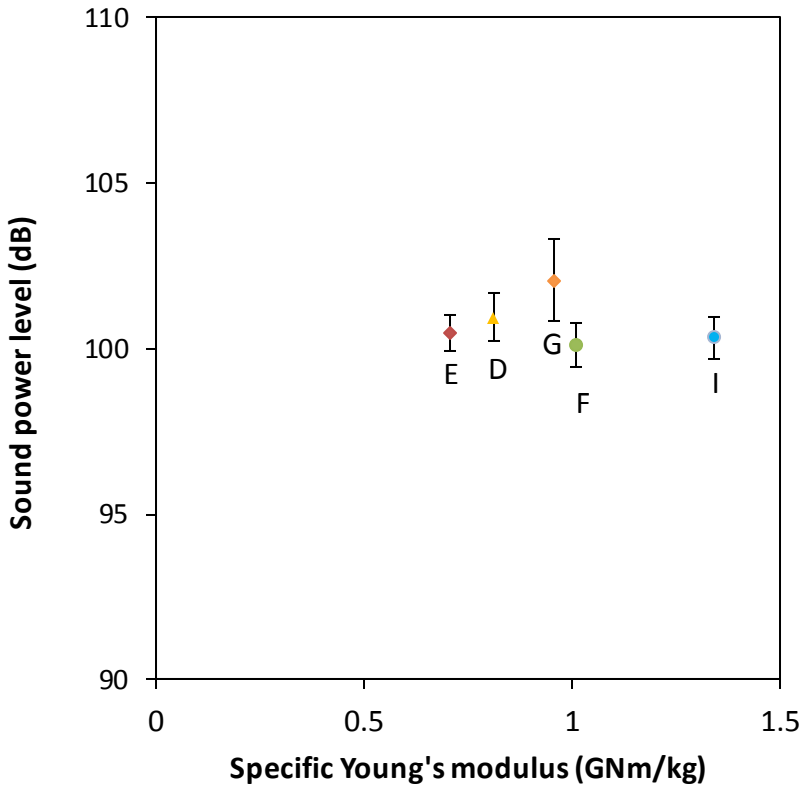

Figure 5 Sound power levels obtained through various types of paper propagating acoustic waves as a function of specific Young's modulus of paper

Figure 2.4 shows the sound power levels as a function of thickness of all the commercially-available paper. With increasing thickness, the sound power level decreased linearly. Consequently, the result implies that paper loses vibration energy with an increase in the propagation distance presumably in the form of heat due to internal friction. Thus, thick paper does not achieve a high degree of efficiency of vibration energy transmission from one side to the other transversely. The combined results from Figures 2.3 and 2.4 suggest that the acoustic waves that propagated laterally as on a beam were not measured; however, those that propagated through different thicknesses of the paper test pieces were measured and the resulting sound power levels were varied from sample to sample.

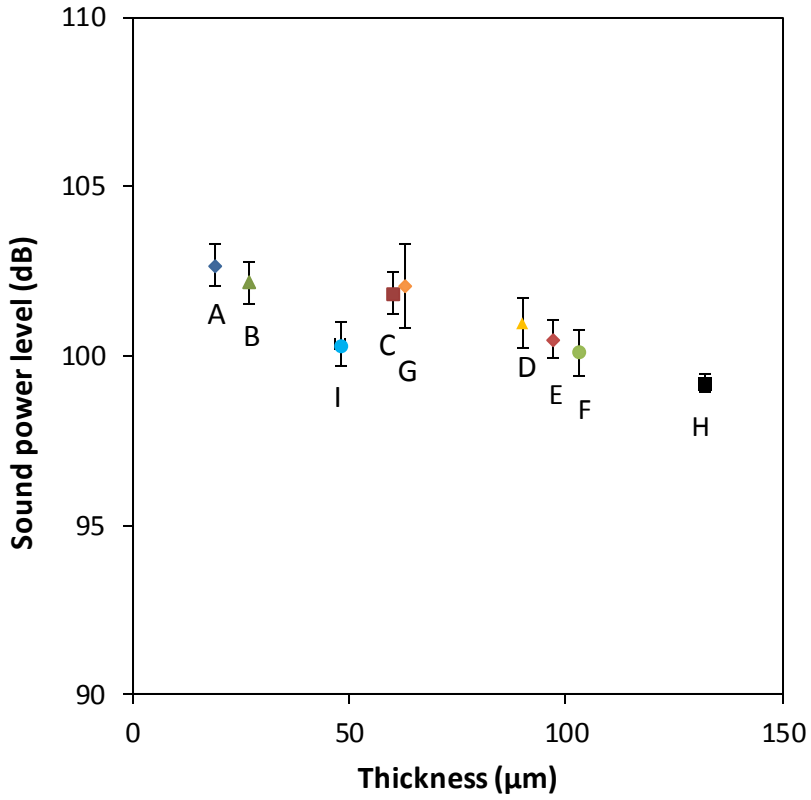

Figure 6 Sound power levels obtained through various types of paper propagating acoustic waves as a function of thickness of paper

Figure 2.5 shows how the density and Young's modulus increase with increasing beating degree for both HBKP and SBKP laboratory sheets. As shown in Table 2.2, four data samples with different grammage class were investigated for each beating degree. The Young's modulus was found to have a linear relationship with the sheet density regardless of the kind of pulp fibers.

Figure 2.6 shows that there is a linear relationship between Young's modulus and the sound power level for the laboratory sheets with a correlation coefficient as high as 0.923 again regardless of the kind of pulp fibers. Note that the range of sound power level is lower than that in Figures 2.3 and 2.4 because the measurement conditions were different.

Figure 2.7 shows that the sound power level had a linear relationship with density and the same relationship applies to both HBKP and SBKP sheets. This tendency is similar to that observed in Figure 2.6.

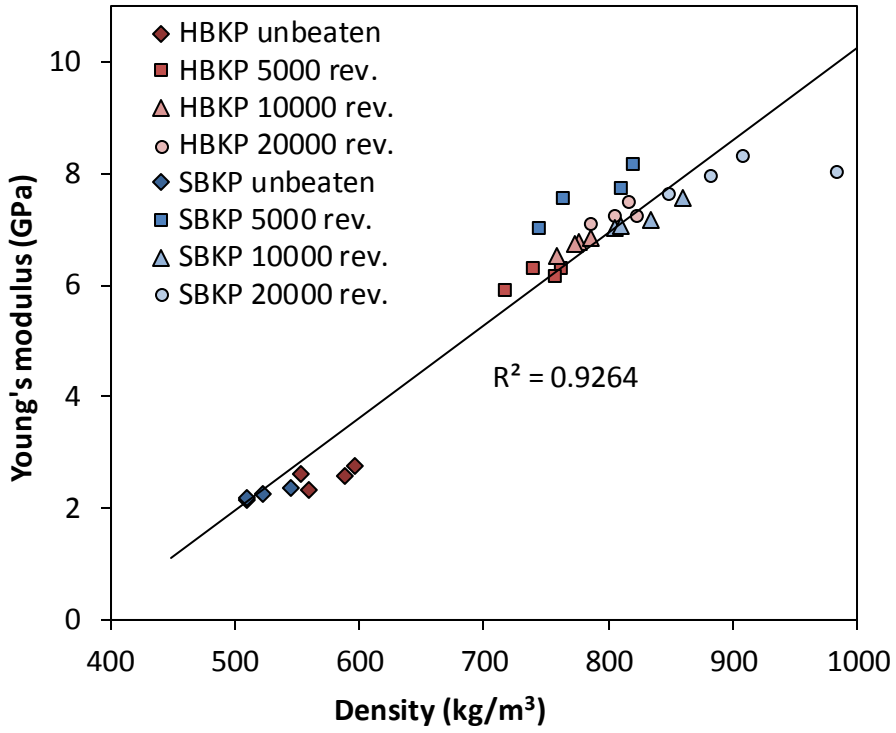

Figure 7 Relationship between density and Young's modulus for HBKP and SBKP laboratory sheets at different beating

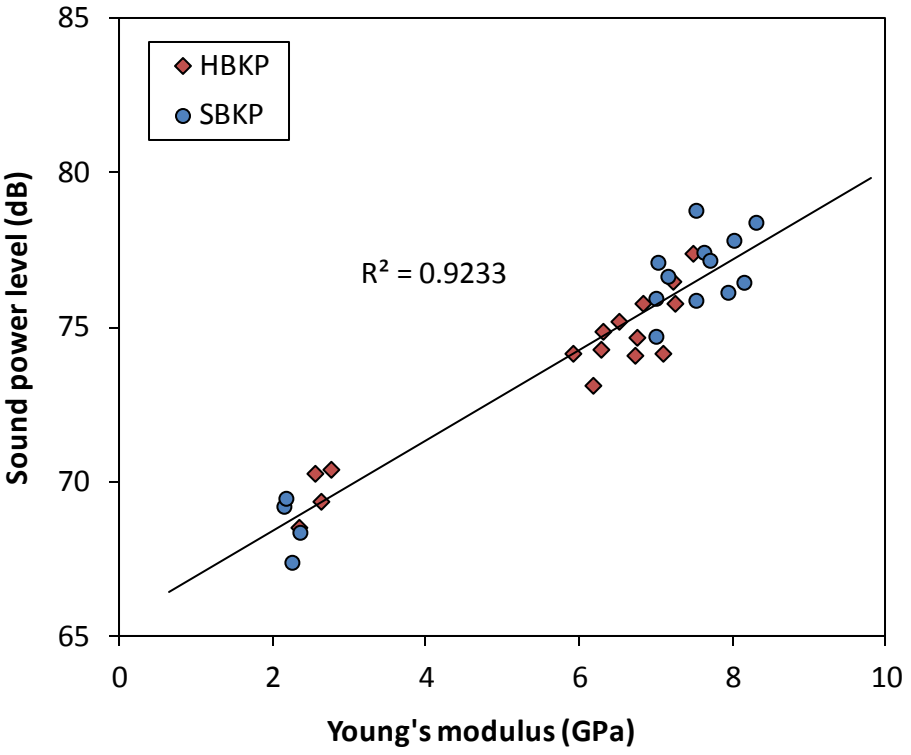

Figure 8 Relationship between Young's modulus and sound power level for HBKP and SBKP laboratory sheets

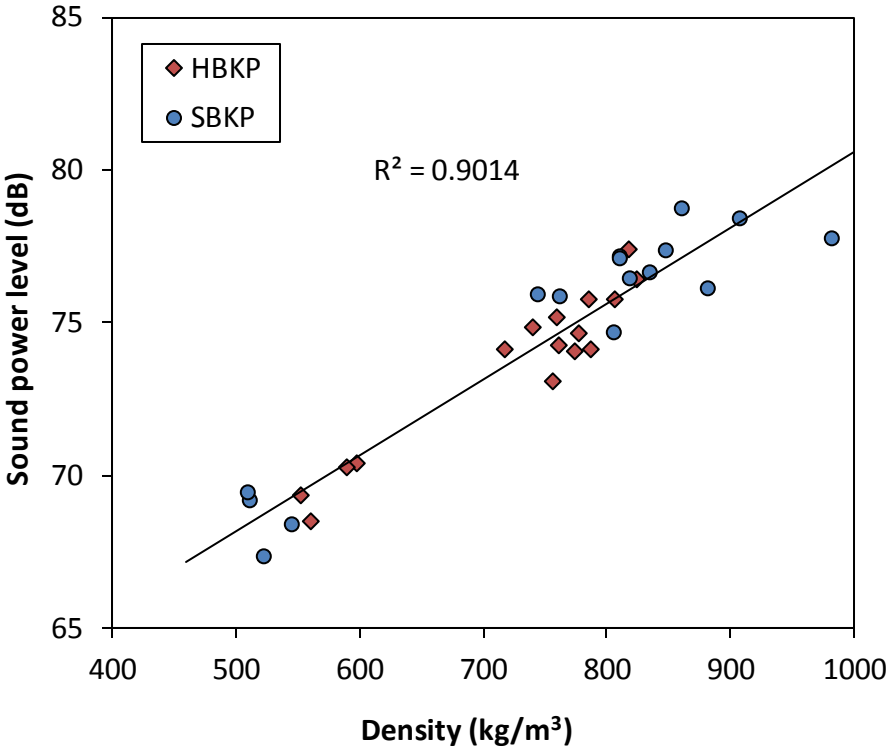

Figure 9 Relationship between density and sound power level for HBKP and SBKP laboratory sheets

Figure 2.8 shows the relationship between the specific Young's modulus and sound power level with a fairly high correlation coefficient of 0.846, as is reasonable considering Eq. (1). Unlike Figure 2.3, sound power level was measured with audible vibration induced by the ultrasonic oscillator. Inaudible ultrasound was considered to change into audible sound by resonance while the vibration propagated along the plane of paper. The vibration propagation could be classified into two modes. For the commercially available paper, the sound was transmitted throughout the thickness of paper (case 1); for the laboratory sheets, the sound propagated in the in-plane or lateral direction (case 2).

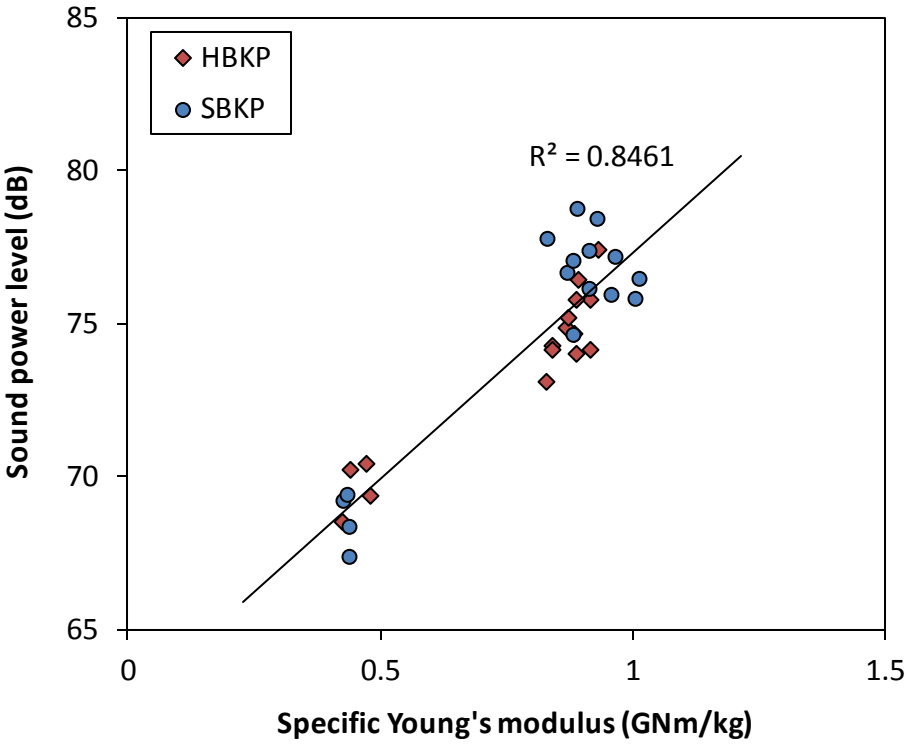

Figure 10 Relationship between specific Young's modulus and sound power level for HBKP and SBKP laboratory sheets

In case (1), acoustic waves that propagate in the air initially and collide against the paper surface and subsequently transmit in the thickness direction as a longitudinal wave. During the transmission inside the paper, compression occurs in the thickness direction. When Young's modulus was tried to be related to the sound power level, Young's modulus in the thickness direction was supposed to be applied. In practice, Young's modulus was measured with the ultrasonic tester. In ultrasonic testing, ultrasonic waves propagate near the paper surface layer probably as plate waves (Haberger, Mann, & Baum, 1979) that include two modes; Rayleigh and Lamb waves (Lamb, 1910). These two modes both vibrate perpendicularly to the propagation direction and Young's modulus in the in-plane direction is determined from the propagation velocity. Figure 2.3 resulted in no definite relationship between Young's modulus and sound power level because of the use of Young's modulus in the in-plane direction.

In case (2), Rayleigh waves vibrating in the thickness direction make compressive waves in air as acoustic waves ; these were to obtain the sound power levels which is why the latter had a linear relationship with Young's modulus for the laboratory sheets. Unlike Challa et al. explained using piezoelectric material that the vibration energy stored in a harvesting device would be changed depending on the frequency as well as the altering mass, length, or thickness of the vibrating structure (Challa, Prasad, Shi, & Fisher, 2008). Therefore, the sound power level is not relevant to the thickness of paper as shown in Figure 2.9 in electret modeling of potential uses of electrostatic vibration energy harvesting.

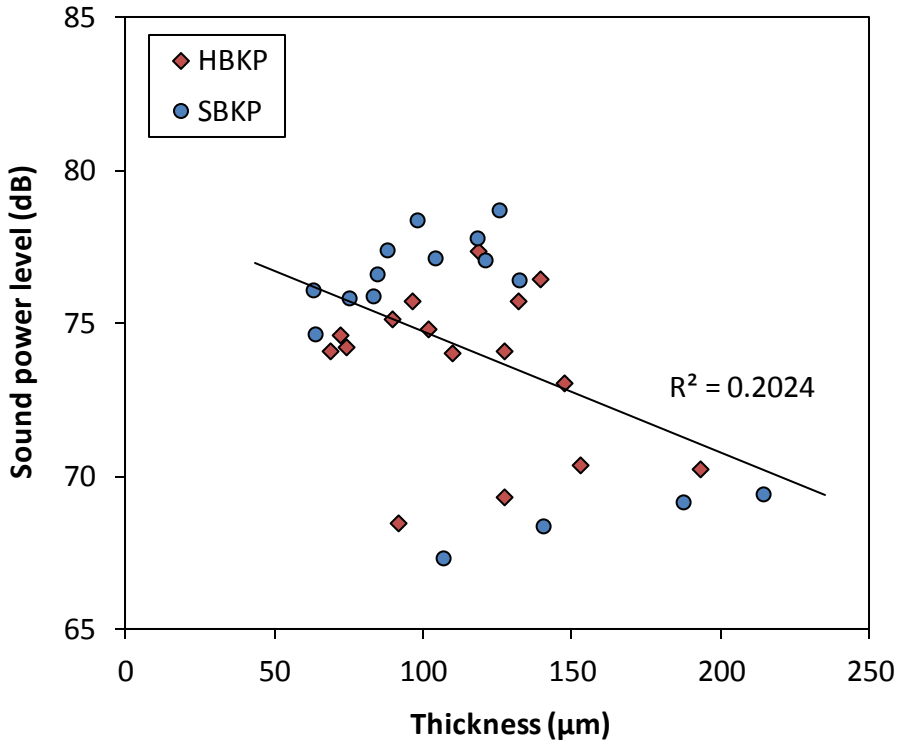

Figure 11 Relationship between thickness and sound power level for HBKP and SBKP laboratory sheets

2.4 Conclusion

The sound power level of acoustic waves after transmission in the thickness direction of the paper was not observed to depend on the in-plane specific Young's modulus; however, it decreased with the increase of paper thickness because longitudinal waves were transmitted through the paper with compression in the thickness direction. Therefore, the vibration energy was damped along the travelling distance. However, when the sound power level was measured with laboratory sheets during ultrasonic testing, the in-plane specific Young's modulus was definitely a key parameter affecting the sound power level. This is because the surface waves propagating near the paper surface in the ultrasonic testing were transverse waves with in-plane compression. Consequently, to efficiently convert vibration energy from environmental noises to electric energy, the damping ratios should be evaluated by considering the traveling and vibration directions. In terms of materials, there was no difference in the vibration damping tendency between SBKP and HBKP.

CHAPTER III

3 RESONANCE OF OUT-OF PLANE PAPER VIBRATION

3.1 Introduction

As an anisotropic material, a machine-made paper can show a high degree of elasticity. Wood as raw material for papermaking has been known for its piezoelectricity in sensor (Ross, Kan, Wang, Blakenburg, Stockhausen, & Pellerin, 2012). The Chladni pattern observation that is one of the typical vibration methods for paper and well-suited for non-uniform and imperfect sheets such as paper and paperboard has been studied (Sato, Hutchings, & Woodhouse, 2008). Paper can displays the highest modulus young as a result of fiber alignment and consequence of stresses during drying. Vibration or sound propagate in paper are related to plate waves. Plate waves mode are abundant, it differs to bulk waves (Tucker, 2001). The dispersive propagation velocity of plate waves depends on frequency (Lamb, 1910).

The power generation mechanisms for transduction from vibration are based on fundamentally inertial-based spring-mass systems with a damper for obtaining resonance movements (Beeby, Tudor, & White, 2006). A micro power generator of the horizontal vibration type was developed and consisted of micro ball bearings in which micro balls rolled with a constant separation gap. For this generator, comb-shaped electrodes were designed and SiO_2 was applied as a proof mass. Vibrations with low frequencies less than 10 Hz resulted in generation of an output power of approximately 100 mW (Naruse, Matsubara, Mabuchi, Izumi, & Honma, 2008). A vertical type of a counter electrode coated with a ferroelectric material has been studied. This counter electrode could generate an output power that increased with increasing capacitance to realize a high surface potential and did not need any comb-shaped pattern. These power generators used

an electret treated with the corona discharge method to inject charge (Takahashi, Suzuki, Nishida, Yoshikawa, & Aoyagi, 2012). Other possible methods of charge injection include triboelectrification and electrostatic spinning (Tsai, Schreuder-Gibson, & Gibson, 2002). However, we chose triboelectrification to charge PTFE films because one sheet of paper with an electrode repeats to hit the other sheet of paper with an electret during vibration and induce triboelectrification. A flexible triboelectric generator (TriboEG) with polyimide (Kapton) and polyethylene terephthalate films has been conducted. Spiral electrode based TriboEG with a bicylindrical structure was designed for harvesting energy of both rotational and translational motions (Guo, et al., 2015). TriboEG was also applied to a self-powered vibration frequency sensor for monitoring machines operation (Liang, et al., 2015).

Meanwhile, paper materials for vibration energy harvesting have not been studied widely. In this work, attention was paid to paper vibration brought out by environmental noise, voice, and sound as an energy source. From several energy conversion mechanisms such as piezoelectric, electromagnetic, and electrostatic systems, we chose an electrostatic system to achieve low weight and compatibility with paper structure. Electret, which consists in a condenser microphone model to take a familiar example, was introduced to this out-of-plane technique. The dynamic stage of microphone is a magnetic omnidirectional constructed with light diaphragm, usually Mylar, the same way as a small loudspeaker. This diaphragm is coupled to a suspended coil in a strong magnetic field. When the diaphragm and coil move together in sympathy with the sound waves, thus an electric current is generated based on Faraday - Lenz law. The law describes some changes in magnetic flux generates electromotive force (emf) using right hand rule (Takahashi, Suzuki, Nishida, Yoshikawa, & Aoyagi, 2012). The vertical arrangement adopted for generators of this type is very popular (Sessler & West, 1962); (Tao, Lye, Miao, & Hu, 2015) and equipped with a membrane functioning as a diaphragm that transfers the vibration to an electric signal. This type has a merit of high enough flexibility in

mechanical design using paper and PTFE sheets. Paper is neutral in terms of electrical charge, and a PTFE sheet acts as an electret. Electret is a dielectric material with permanent negative electric field that is achieved by rubbing it with another paper. Paper is also applicable to the system for transmission of mechanical movement to an electret. The origami structure works like a spring to transmit energy of stretching, lifting, and twisting motions (Yang, et al., 2015).

The current study reports the trial simulation data for future application of paper vibration due to environmental noise, voice, and sound as an energy source with voltage obtained from a prototype paperboard TriboEG. In this system, the weight and elasticity of paper in itself function as a proof mass and spring, respectively. During vibration, the paper keeps energy and it immediately transfers to electricity via electrostatic induction.

3.2 Experimental

There are 2 directions in which the displacement of the medium when a sonic wave travels through the medium such as paper. The 2 modes of waves are called longitudinal and transverse waves consisting of the oscillations occurring parallel and perpendicular to the direction of the propagation, respectively. The ratio of the 2 waves is related to the moduli of elasticity and rigidity. Two types of electrostatic vibration energy harvester were fabricated corresponding to the 2 waves so that the relative motion of an electret to the counter electrode is out-of-plane and in-plane.

3.2.1 Materials

Paperboard was applied as both a sound propagation material and substrate to support an electret and electrodes. PTFE (Du Pont, USA) and copper tape with electroconductive acrylate adhesive

(CCH, Chomerics, USA) for an electret and electrodes, respectively. Table 3.1 shows physical properties of those materials for fabricating the paperboard TriboEG.

Table 3.1 Condition of the paperboard triboelectric generator (out-of-plane motion)

Material	Property	Value
Paperboard	Grammage (g/m^2)	736
	Thickness (mm)	1.13
	Dimension (mm×mm)	90×209 (Fixed part)
		90×153 (Moving part)
	Gap between fixed and moving parts (mm)	1 and 2
PTFE	Thickness (mm)	0.50
(Electret)	Dimension (mm×mm)	40×40
Copper	Thickness (mm)	0.036 (copper)
(Electrode)		0.038 (conductive
		adhesive)
	Dimension (mm×mm)	25×125

3.2.2 Method- Corona Treatment

To charge the electret material, it was treated with corona discharge as shown in Figure 3.1 in this experiment. A high voltage corona discharge treatment (GC50S, Green Techno, Inc, Japan) with a bias needle voltage of -50 kV was applied back and forth 30 mm away from the surface of

a PTFE electret with an area of 23000 mm^2 and a thickness of 0.5 mm before attaching it on the paperboard TriboEG.

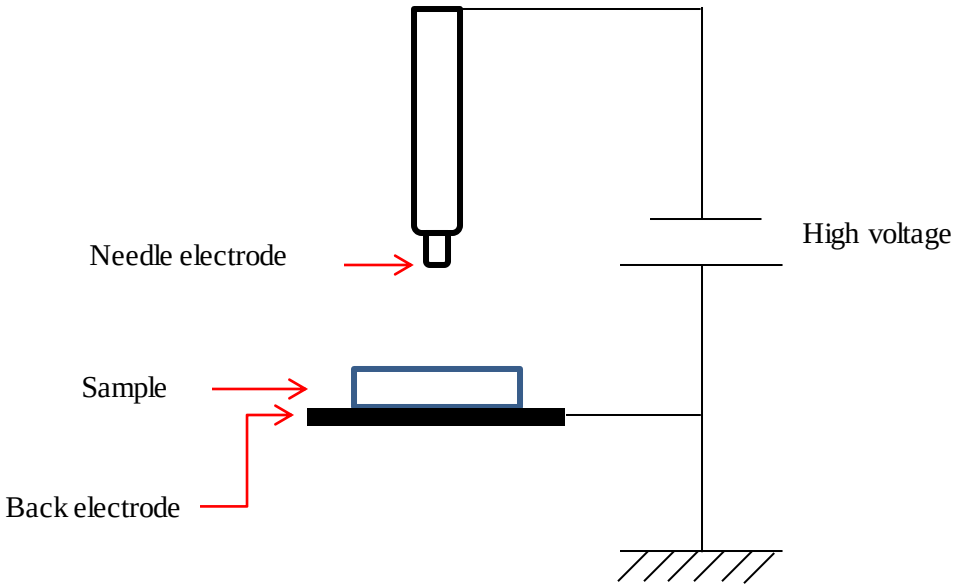

Figure 12 Corona treatment scheme

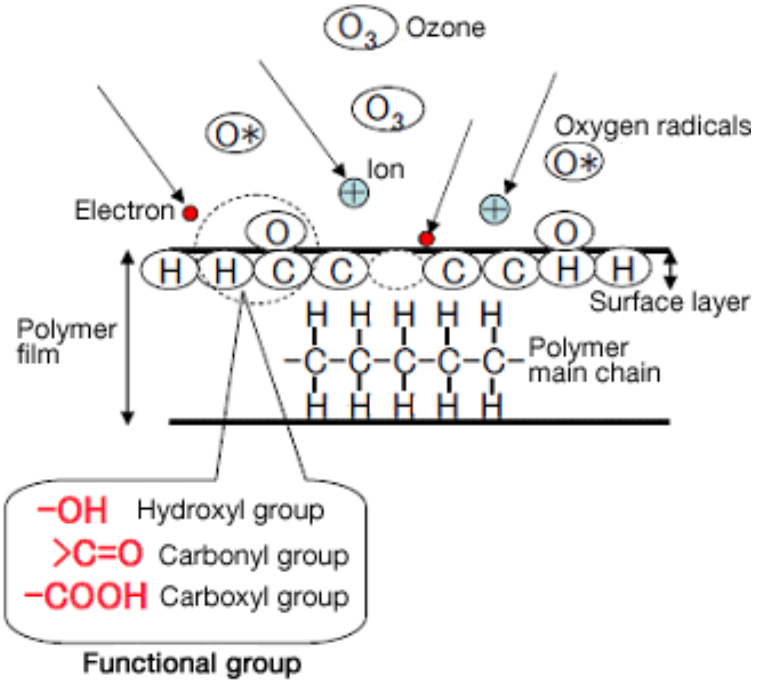

Figure 13 Surface modification during corona treatment (Kasuga Denki, Inc., 2012)

Figure 3.2 shows surface modification during corona treatment (Kasuga Denki, Inc., 2012). High voltage generates high energy electrons that reach the surface layer of a polymer sample, thus triggers an action that cut outs the main chain or side chains of the polymer. The polymer surface layer becomes chemically radical, and when oxygen radicals or the ozone layer in the gas phase are combined with the main or side chains, a polar functional group such as the hydroxyl group or carbonyl group is introduced to the surface and made it hydrophilic. This improves the printing property, adherence property, lamination, and thus benefits the packaging field (Lahti & Tuominen, 2007). The surface modification does not extend more than 0.1 μm in depth, thus the corona treatment would not affect the properties of the base material of samples.

Figure 3.3 shows surface potentials of PTFE sheets rubbed against copy paper for 1 min, corona-discharge-treated, and untreated for comparison. The charge density of electrets has been reported to be improved significantly with a high bias needle voltage (Lee & Chiu, 2011). The default voltage -50 kV of the corona discharge in this work was high enough. Thus, the discharge time was set to 2 min and the surface potential started to be measured 1 min after discharge with a surface potential meter (digital static meter KSD-2000, Kasuga Denki, Inc., Japan).

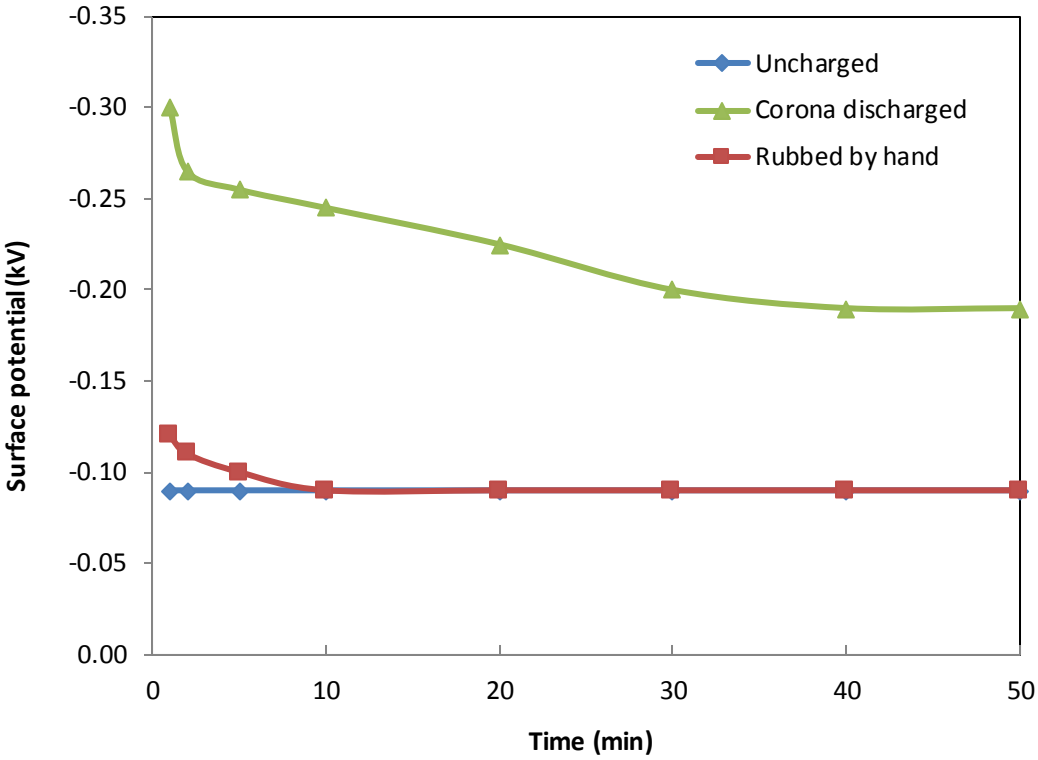

Figure 14 Surface charge of PTFE sheet

The surface potential of the untreated sheet was -0.09 kV. It was found that the rubbed PTFE sheet was provided with a high negative surface potential and kept it higher than the untreated for only about 10 min. Therefore, continuous rubbing action is required to keep the potential. Although the corona-discharge-treated PTFE sheet shows a rapid decrease in the negative potential for initial 30 min, it still kept a much higher negative charge than the rubbed PTFE sheet. Thus, corona-discharged PTFE sheets can be applicable to active power generation. In electrochemical experiments, however, electrostatic charges on rubbed PTFE sheets were directly identified as electrons rather than ions (Liu & Bard, 2008). The realization of this prototype dielectric material is suitable for interactive power generation.

3.2.3 Fabrication of the paperboard

Figure 3.4 shows the design configuration of the paperboard TriboEG with an out-of-plane motion. Both the fixed and moving parts of the two paperboards were mounted on a stand such that the periphery would not be shifted and the narrow gap between the two paperboards would be maintained. To design the paperboard TriboEG, the condenser microphone structure was introduced. The vertical arrangement of this structure, which is popular for microphone applications, was equipped with a membrane functioning as a diaphragm to transfer sound-induced vibration into an electric signal via dielectric polarization. One of the advantages of this structure is its high flexibility and its applicability to paper and PTFE sheets. Paper is neutral in terms of the electric charge. A PTFE sheet functions as an electret because it is a dielectric material with a permanent negative electric field created by corona discharge or simply rubbing it with another triboelectric material.

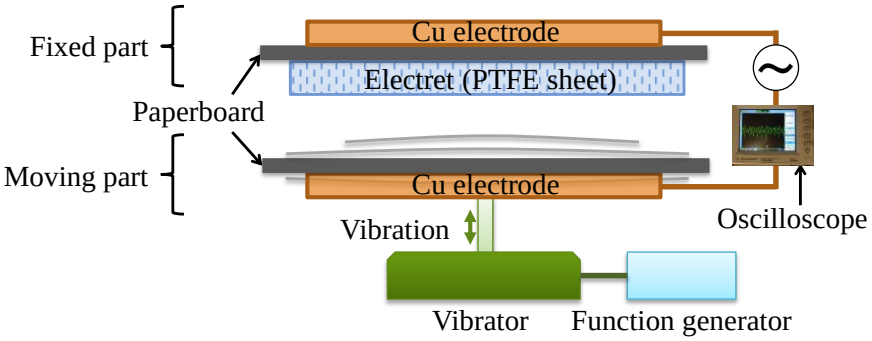

Figure 15 Design configuration of the paperboard triboelectric generator (out-of-plane motion).

3.2.4 Preliminary test- Adjustment of vibration amplitude at various frequencies

The vibration generator showed different amplitude of vibration. It is necessary to maintain the constant amplitude of vibration of the vibration generator. In this subsection, the vibration behavior of a paper sample was recorded and the adequate voltage output from a function generator was tried to be determined to stabilize the vibration amplitude. This setting was conducted without using any paper sample as illustrated in Figure 3.5 to obtain the constant vibration amplitude of the tip point by varying the voltages range (1 to 20 in Vp-p) at vibration frequencies ranging from 1 to 65 Hz.

The sampling rate of the laser profilometer to monitor the displacement during vibration was set to 200 Hz.

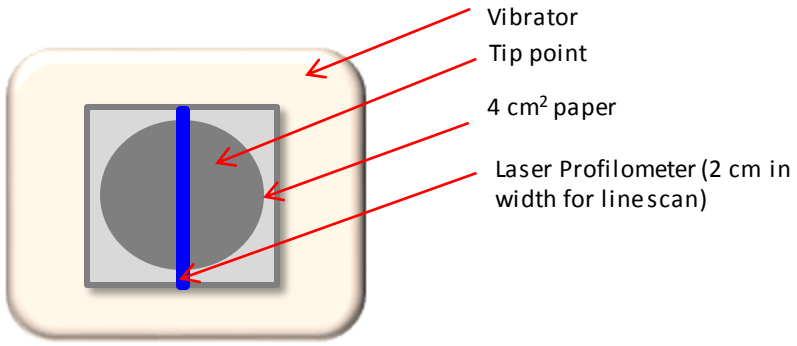

Figure 16 From top view. Sampling position placed on top of tip point

Figure 3.6 shows relatively the same amplitudes of vibration at given frequencies and input voltages by the multifunction generator. The FFT analysis of average data shows that the vibrational displacement of the tip point varies between 0.0125 mm to 0.1149 mm. The standard deviation was 0.0300 mm. Subsection 3.2.3 will report the displacement of paper edges at the same frequencies and input voltages applied in this subsection.

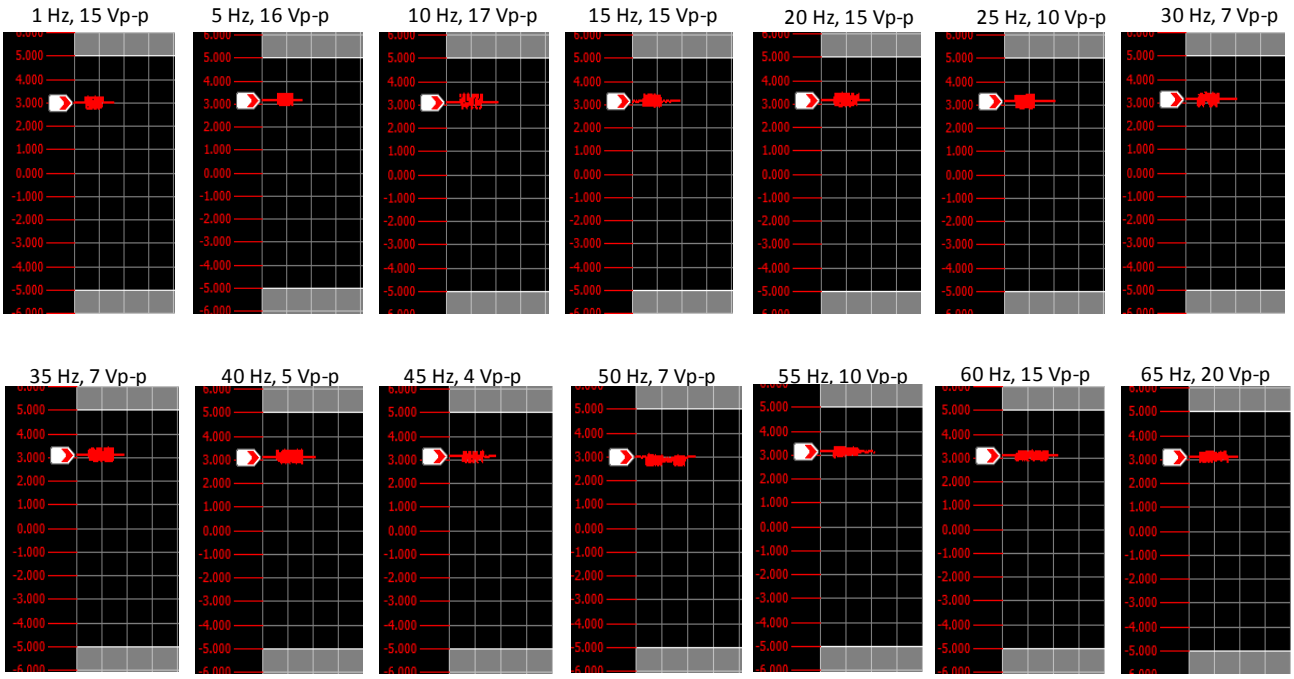

Figure 17 Observations of tip point displacements at various frequencies and voltages by multifunction generator.

3.2.5 Profile of paper surface during vibration

An A4 size copy paper (0.06 mm-thick, up to 70% recycled fibers, Mitsubishi Paper Mills) was used in a test in order to obtain the behavior of the transient displacement of a paper edge at various frequencies of vibration using the profilometer. Figure 3.7 shows the experimental setup for the displacement measurement of a paper sample supported centrally with free edges without tension in the vertical arrangement.

This experiment used a vibration generator (U56001, 3B Scientific Physics), multifunction generator (WF 1973, 300 MHz, NF), profilometer (LJ-V7000, Keyence) with a laser head (LJ-V7060, Keyence), and two-axis stage controller (QT-ADM2, Chuo Seiki) with the standard driver (QT-AK, Chuo Seiki). The sampling rate of the profilometer was set at 200 Hz. This sampling rate must be at least twice higher than that of paper vibration in order to cover the broad band sampling, that is, every possible frequency. A laser head for a 20 mm-line profile was directed to an area close to one edge of the vibrating paper sample. The paper displacement was analyzed using fast Fourier transform (FFT).

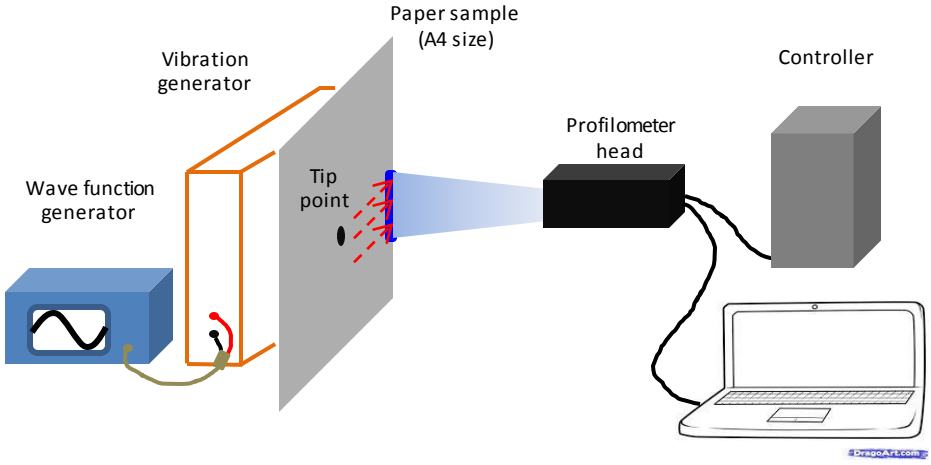

Figure 18 Arrangement of paper sample and apparatus for displacement measurement

3.2.6 Data acquisition of voltage and power generated by the paperboard TriboEG

To vibrate the moving part, a vibration generator (U56001 Vibration generator, 3B Scientific Physics, Germany) with a signal source from a multifunction generator (WF1973, NF Corporation, Japan) was used for the TriboEG (out-of-plane motion). To record the generated voltage, an oscilloscope (DSO1052B, Agilent Technologies, USA) was used for both the out-of-plane and in-plane motion modes. The voltage generated by the forced vibration from the vibration generator was recorded by the oscilloscope under the conditions shown in Table 3.2 and analyzed using fast Fourier transform (FFT) to determine the natural frequency of the paperboard and separate the generated electricity from the electric noise sourced by the power outlet in the room. The FFT calculation was conducted by using the analysis function of a spreadsheet application (Excel 2010, Microsoft Corp., USA). As shown in the next chapter, each Fourier coefficient (amplitude) of the background wave was subtracted from those of the measured voltage waves at every frequency in the Fourier space.

Table 3.2 Data acquisition system of generated voltage

Instrument	Property	Value
Vibration generator and multifunction generator	Frequency (Hz)	Background,10, 20, 30, 40, 46, 50 and 55
	Amplitude $V_{p\text{-}p}$ (V)	10
Oscilloscope	Amplitude (V)	2
	Sampling rate (Hz)	500
	Recording period (s)	1.024

3.3 Results and Discussion

Figure 3.8 shows recorded voltage at each frequency of forced vibration and Figure 3.9 shows FFT analysis of voltages after normalized with background, generated by the 2 sheets of out-of-plane paperboard at a gap between fixed and moving parts of 2 mm. The background noise consisted of a 51-Hz sinusoidal wave. (The specified frequency of a commercial power source in eastern Japan is 50 Hz). Therefore, all generated voltages include this background noise. There were similar resonance between set vibration frequencies and vibration movement of paperboards. The highest voltage up to 2.3 V was produced at 46 Hz of vibration spectrum that resonating with 46 Hz of natural frequency.

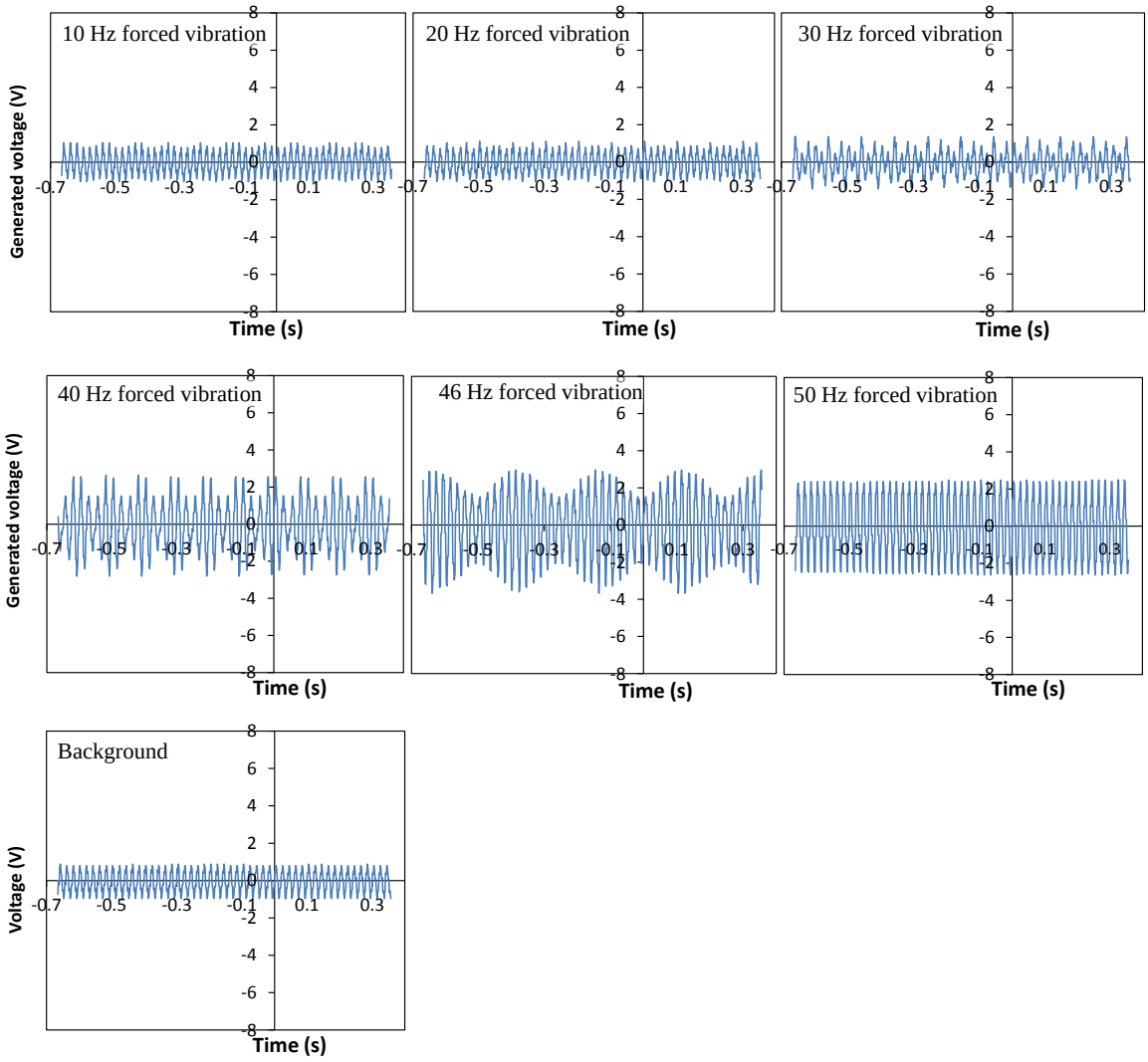

Figure 19 Voltages generated by paperboard triboelectric generator at a gap of 2 mm and voltage of background electric noise

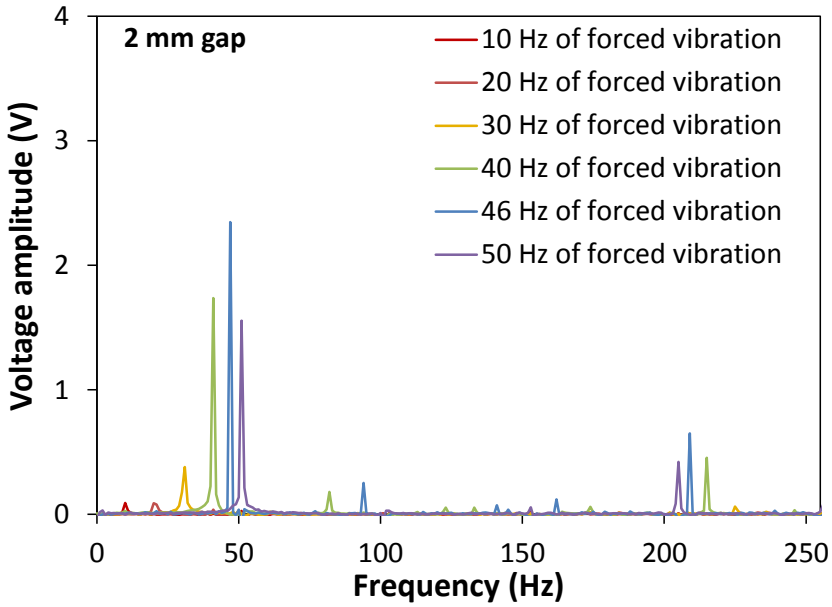

Figure 20 Spectra of voltage amplitude generated by paperboards at a gap of 2 mm with background noise

A gap between the fixed and moving parts is desired to be as small as possible for effective energy generation by static electricity (Takahashi, Suzuki, Nishida, Yoshikawa, & Aoyagi, 2012), (Naruse, Matsubara, Mabuchi, Izumi, & Honma, 2008). At narrower gaps, the paperboard – PTFE generator generated higher voltages as shown in Figure 3.10 and 3.11. This energy generation will be effective especially at vibration frequencies higher than 30 Hz. At 30 Hz, the 1 mm gap configuration generated almost 2 times that of the 2 mm gap. There are also advantages of decreasing interference at 51 Hz, if there is, from electrical source background. The voltage peak in the 46 Hz vibration spectrum achieved the highest power, i.e., approximately 3.5 V. In the 50 Hz vibration spectrum, the voltage peak attained at a quite high voltage of 2.8 V. Respectively, in the same spectrum of 46 Hz and 50 Hz, another large peak with a height of approximately 2.0 V was observed at 24 Hz and 26 Hz. In the 55 Hz vibration spectrum, the peak voltage at 56 Hz was lower than the peak at 47 Hz in the 46 Hz vibration spectrum. The maximum resonance seems to appear at around 46 Hz in applied vibration frequency. Consequently, this measurement method seems suitable for characterizing the vibration mode and relating to paper properties for the maximum efficient energy harvesting at frequencies as low as a few tens of Hz from environmental sources. The power determination (see Appendix) using several load resistances shows a maximum power of 11.8 μW at 2 MΩ and 39 Hz.

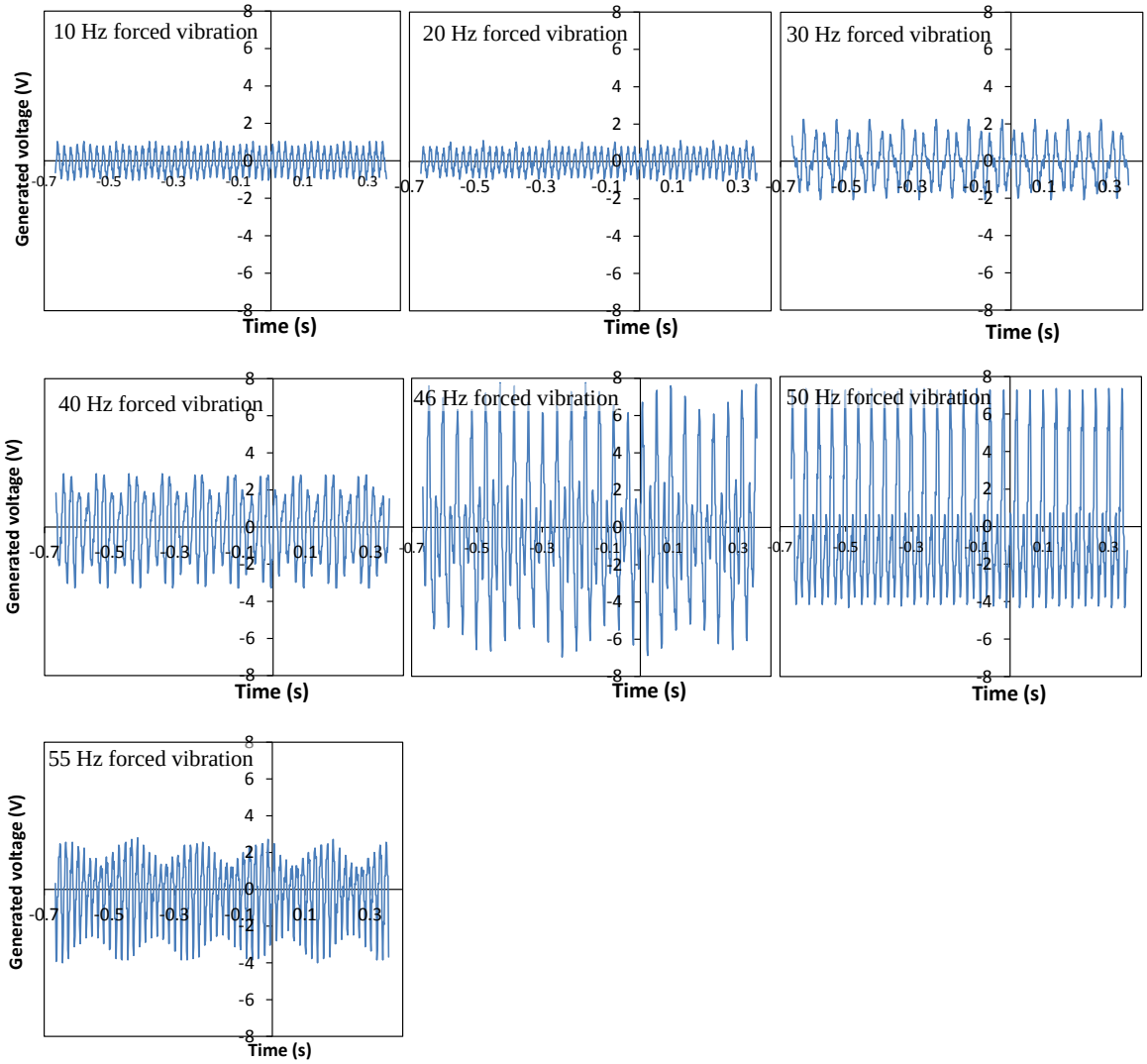

Figure 21 Voltages generated by paperboard triboelectric generator at a gap of 1 mm and voltage of background electric noise

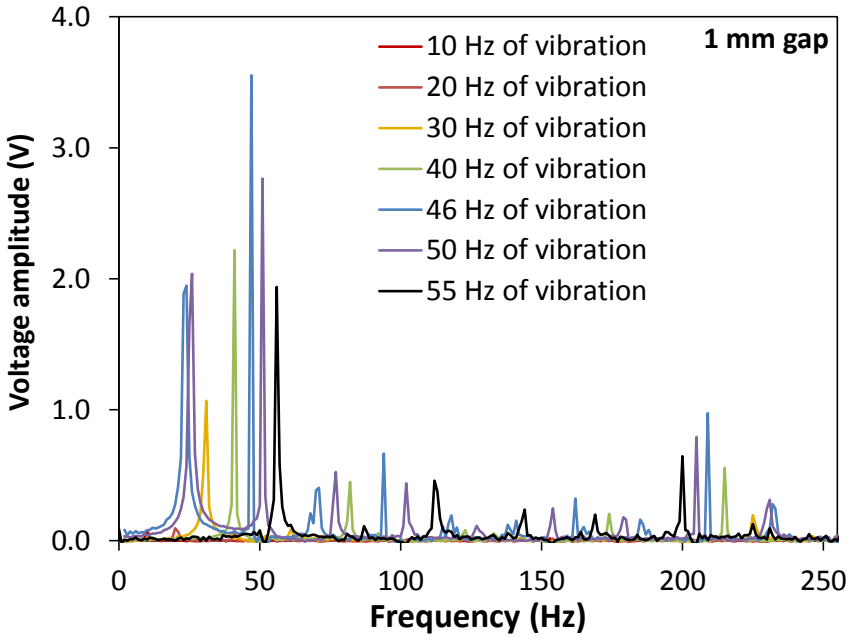

Figure 22 FFT analysis of voltages generated by paperboards at a gap of 1 mm

Study on vibration behavior of paper has not been reported much thus far. Paper is an anisotropic material, thus the vibratory or sonic properties are supposed to depend on the direction. Figure 3.12 illustrates the line profile location in a paper sheet. Figure 3.13 shows no significant differences on the displacement of vibrating a A4 format copy paper sheet measured in machine and cross directions, respectively, relative to the height of the laser head of the profilometer. Vibrations are the same in machine and cross direction since supporting point was in the center of paper sample. These results are similar to the conclusion by Jun Sato et al.

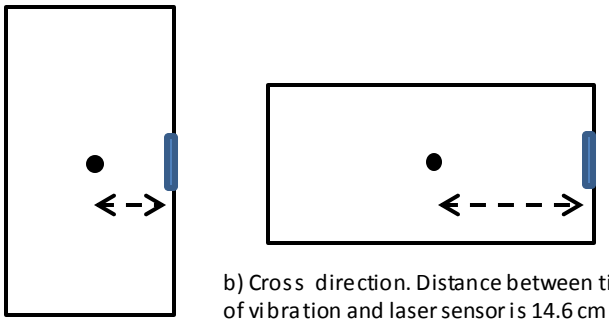

a) Machine direction. Distance between tip point of vibration and laser sensor is 11.5 cm

b) Cross direction. Distance between tip point of vibration and laser sensor is 14.6 cm

Figure 23 Illustration of line profile location in paper sheet

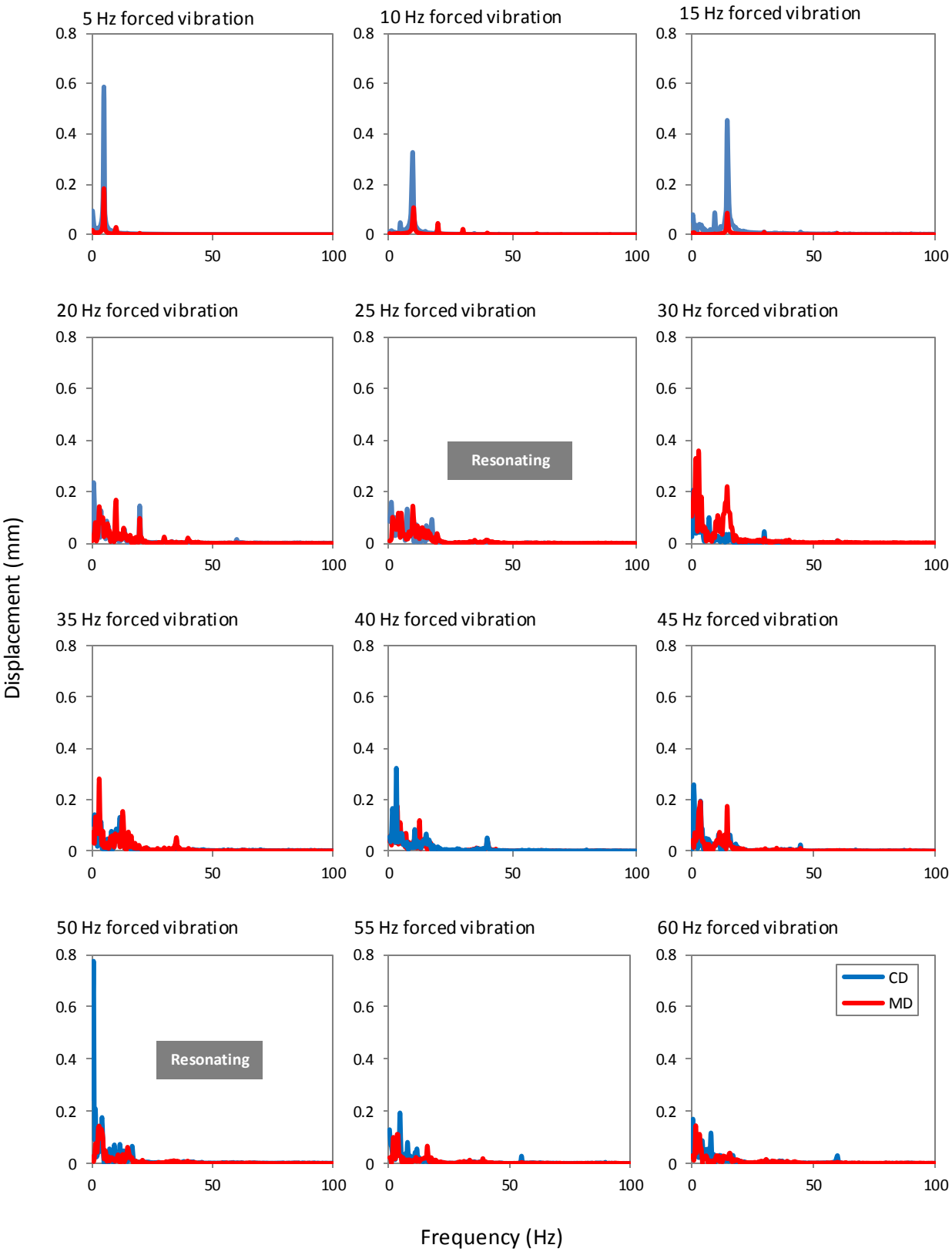

Figure 3.13 Paper vibration displacement in machine direction and cross direction

The frequencies calculated by FFT analyses for the copy paper in both machine and cross directions resulted in shifts from the vibration frequencies set based on the peak of paper displacements in the former experiment. The calculated resonance frequencies were 1.17 , 5.08 , 10.16 , 14.84 , 19.92 , 30.08 , 35.16 , 39.84 , 44.92 , 55.08 , 60.16 , and 64.84 Hz. The resonance peaks were observed at shifted frequencies near 25 and 50 Hz. This finding is probably due to overtone frequencies, destructive interference of half phase and one phase of electrical background.

At shifted frequencies of machine direction in figure 3.13, the high paper displacement was 0.59 mm at 5 Hz of vibration frequency, and matched with the calculated vibration frequency by FFT analysis, i.e., 5.08 Hz. On the other hand, the high resonance displacement was 0.77 mm at 0.78 Hz of force vibration in cross direction. with no resonance at the force vibration frequency. The positions of cellulose fibers in machine direction relative to the profile line were more uniform compared with cross direction. Figure 3.13 suggested that the highest paper displacement was obtained at a lower frequency, i.e., 5 Hz. Consequently, the paper displacement was independent to the voltage generation presumably because other parameters such as paper dimension and tension were not considered.

3.4 Conclusion

Electric energy could be generated using a simple TriboEG with paperboard as a vibration transmission medium and PTFE as an electret. The final purpose of this research was to convert sonic waves such as environmental noise, voice, and sound to electric energy. Based on the dual wave nature of sound in which longitudinal and transverse waves propagate in a solid material, two types of TriboEGs were established in the out-of-plane and in-plane modes. These TriboEG systems successfully generated the voltage amplitude of 3.5 V at a forced vibration frequency of 46 Hz. In addition, the paper displacement was independent of voltage generation or more likely related to vibration frequency because other parameters such as paper dimension were not considered.

CHAPTER IV

4 RESONANCE OF IN - PLANE PAPER VIBRATION

4.1 Introduction

In this chapter, in-plane electrostatic induction introduced as another type of vibration harvesting energy. In-plane vibration has been an interest widely to many researchers as well as out-of-plane mode. Development of nano–micro power generation of the sliding type focused among them (Boisseau, Duret, Chaillout, & Despesse, 2012); (Sakane, Suzuki, & Kasagi, 2008); (Matsumoto, Saruwatari, & Suzuki, 2012) ; (Naruse, Matsubara, Mabuchi, Izumi, & Honma, 2008) and other type is rotational (Genda, Tanaka, & Esashi, 2004); (Boland, Chao, Suzuki, & Tai, 2003).

Working with ambient environment to harvest vibration energy at lower than 100 Hz input frequency usually requires small-scale device, thin and long guide beams (Boisseau, Despesse, & Seddik, Electrostatic conversion for vibration energy harvesting, 2012). This limitation is a challenge for paper product to overcome some drawbacks. Unlike silicone base material for MEMS, paper can be made from small scale to large scale, form roll-to-roll into plane production.

This work aims to study the efficient transfer of energy held in paper as vibrations from environment. The vertical arrangement adopted for generators of this type is very popular and equipped with a membrane functioning as a diaphragm that transfers the vibration to an electric signal. This type has a merit of high enough flexibility in mechanical design using paper and PTFE sheets. Paper is neutral in terms of electrical charge. A PTFE sheet acts as an electret.

Electret is a dielectric material with permanent negative electric field that is achieved by rubbing it with another paper. In this chapter, the technique of comb-shape patterning is included. Electret has been used effectively in cooperation with micromachining technology for electrostatic self-powered devices (Hsu, Hsich, Tai, & Furatani, 1996). Some researchers has been developed a micro electret generator with a 15 μm thick film of specialized perfluoropolymer with a charge density of 1.37 mC/m^2 that is higher than that of PTFE (Arakawa, Suzuki, & Kasagi, 2004); (Tsutsumino, Suzuki, & Kasagi, Electromechanical modeling of micro electret generator for energy harvesting, 2007); (Tsutsumino, Suzuki, Kasagi, Kashiwagi, & Morizawa, 2006, 2006). Harvesting energy from wind using triboelectric mechanisms was already confirmed with a system in which flexible gold-coated fabrics fluttered against a rigid gold-coated counter plate as a counter electrode with a PTFE film, giving an average power density of approximately 0.86 mW (Bae, et al., 2014).

4.2 Experimental

4.2.1 Sliding type generator

A poster paper sample 150 g/m^2 in grammage was tested in this work. Paperboard was used as a supporting material to provide stiffness during vibration. A PTFE electret sheet with a thickness of 0.5 mm as the moving part was attached on the top of another poster paper of the same type and a 6 array comb-shaped copper tape was additionally attached on the bottom. The teeth of the comb electrode were each 7.5 mm x 99 mm in dimension. Two copper tape electrodes with the same shape, i.e., 12 array comb shape were attached to poster paper as the fixed part. High voltage was expected to be generated due to repeated strokes by manual operation. Two sliding rails were used to provide the stable movement of the moving part on the track during vibration.

In this experiment, the manual operation substituted for the vibration and multifunction generators as detailed in Table 4.1.

The propagation of a longitudinal wave was taken into account and the in-plane motion mechanism was designed using comb-shaped electrodes. Figure 4.1 shows the in-plane design configuration of the paperboard (not to scale).

The voltage generated by the forced vibration from the vibration generator was recorded with time and analyzed using FFT to find the frequency with a maximum voltage in this paperboard condition and separate the generated electricity from an electric noise sourced from the power outlet of the room.

Table 4.1 Data acquisition system of generated voltage

Operation	**Property**	**Value**
Manual forced vibration	Frequency (Hz)	Slow and fast as recorded in oscilloscope
Oscilloscope recording	Amplitude (V)	2
	Sampling rate (Hz)	500
	Recording period (s)	1.024

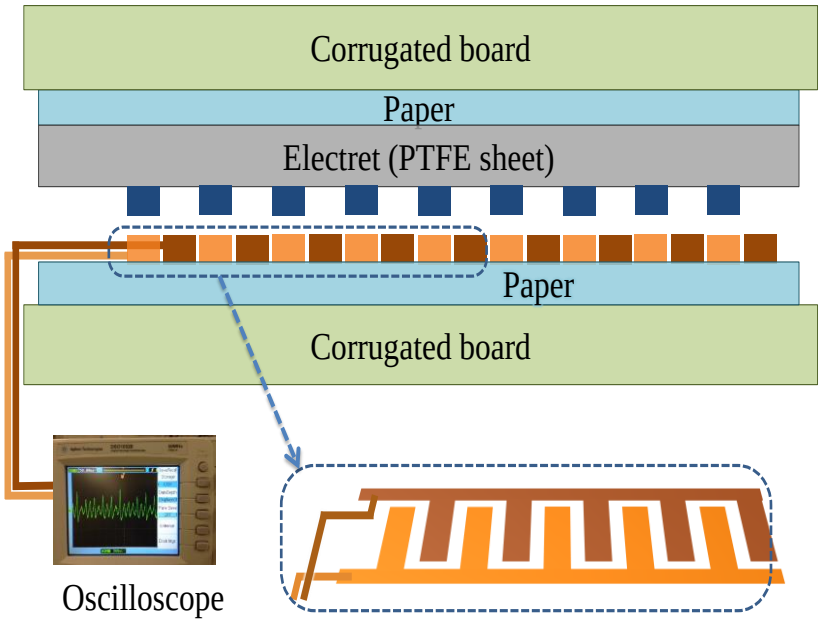

Figure 24 Design configuration of the sliding type paper-based generator

4.2.2 Rotating type generator

Poster paper sample 150 g/m^2 was tested in this work. Corrugated board was used as a supporting material to provide stiffness during rotation. A PTFE electret sheet with a thickness of 0.5 mm as the moving part was attached on top of another poster paper as shown in Figure 4.2.

As the moving part, a PTFE electret was cut to the same size as the outer electrode. Figure 4.3 shows a top view of the fixed part. Unlike the sliding type, the rotating type differs between inner and outer electrodes. Each electrode has 16 arrays of comb-shape patterning connected to the oscilloscope. The outer electrode diameter was 70 mm, and the largest width of the electrodes was 10 mm. Experiments were conducted at various rotation rates of the drill motor as shown in Table 4.2 .

Table 4.2 Data acquisition system of generated voltage of rotating type

Operation	**Property**	**Value**
Motor rotation	rpm	10, 26, 46, 70, 125, and 178
Oscilloscope recording	Amplitude (V)	2
	Sampling rate (Hz)	500
	Recording period (s)	1.024

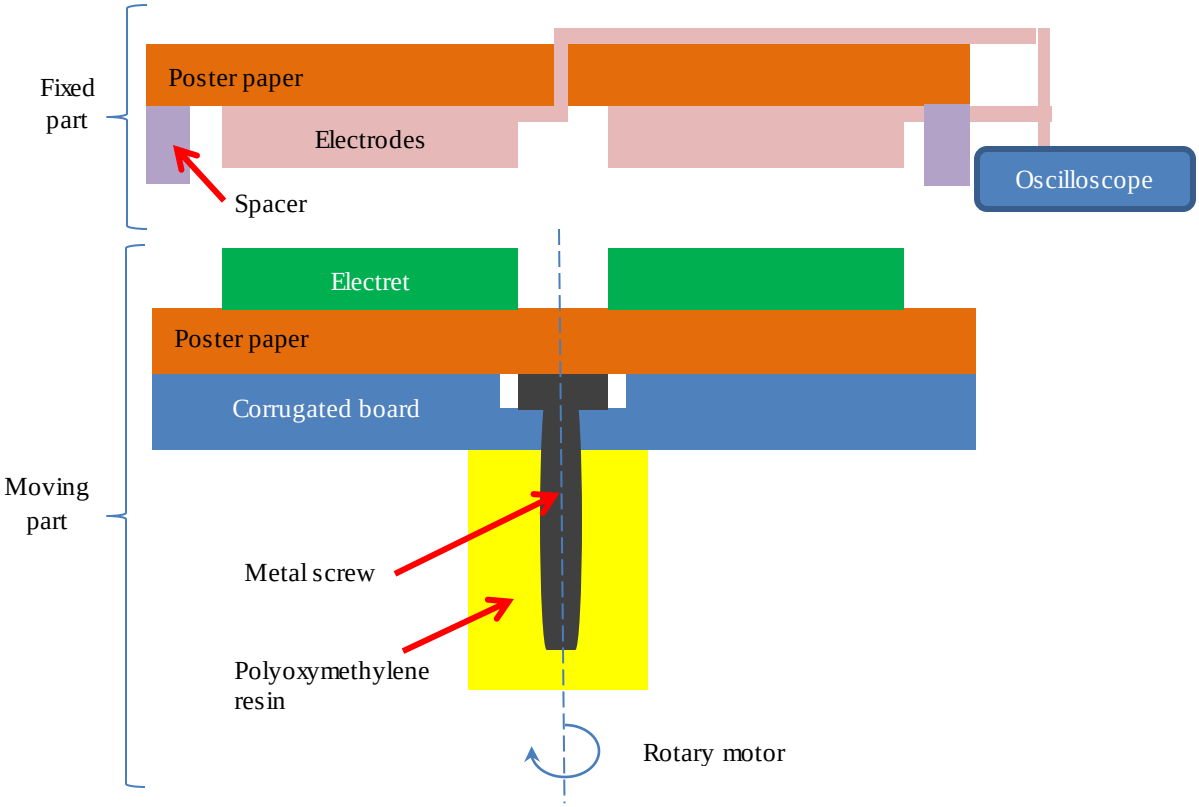

Figure 25 Rotating type for vibration energy harvesting

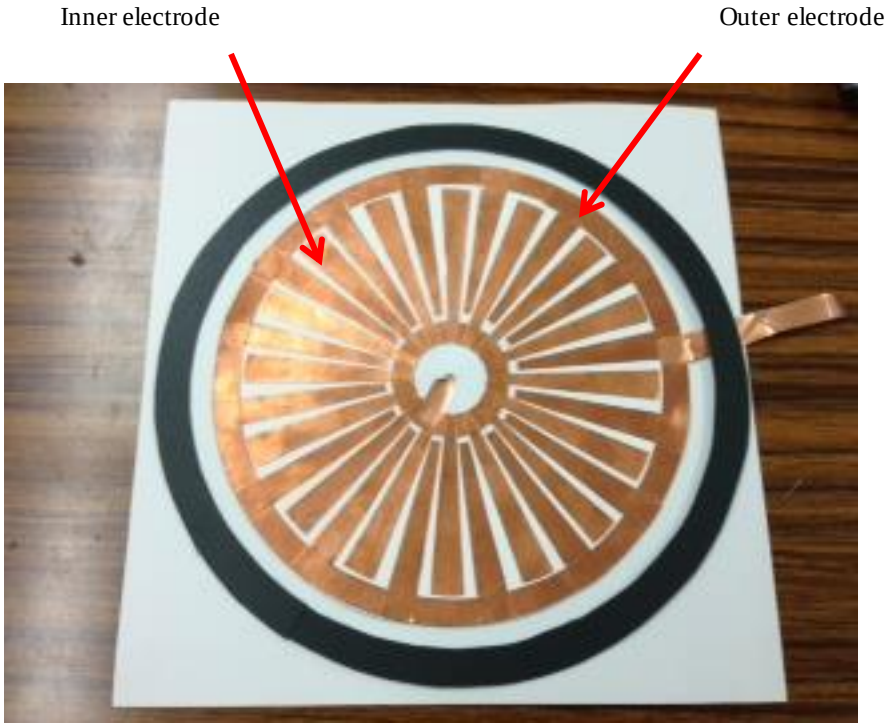

Figure 26 Top view of moving part of rotating type

4.3 Result and Discussion

4.3.1 Output voltage of sliding type generator

Among three gap levels set for this experiment, the narrowest gap, i.e., 1 mm resulted in the highest voltage generation as shown in Figure 4.6. Comparing to the tapping mode of out-of-plane in Chapter III, the in-plane vibration can generate higher voltages. This is due to the comb-shaped electrodes that resulted in a higher surface charge and larger electron flow between the two line electrodes. The paperboard TriboEG system for in-plane motion generated voltage with a sliding action by hand as shown in Figures 4.4, 4.5 and 4.6 with a gap of 3, 2 and 1 mm between the paperboards, respectively. Each of the three large-scale pulse waves was found to consist of 12 oscillations, corresponding to the number of teeth of the comb-shaped electrodes during two cycles of the stroke. The generated voltage wave to the left of Figure 4.6 shows a similar tendency except for the much larger amplitude caused by the higher changing rate of the electric field induced by the narrower gap. The generated voltage momentarily reached 1.3 and 8.2 V at 3 and 1 mm gaps, respectively. The FFT amplitudes to the right of those figures show the highest peaks at approximately 60 to 70 Hz. Those frequencies depended on the moving speed of the examiner's hand and the interval of the electrode teeth. Practical longitudinal waves of sound are weak, and their displacement is much smaller than that in this experiment. However, this result proved that in-plane displacement can generate electricity. The power generation (see Appendix) of sliding type using bridge rectification and Zenner diode shows 8.684 nW. This result further indicated that microscopic electrodes and electret-printed two sheets of paper with smoothly finished surfaces at a high resolution could be an electric power source for microscopic electronics.

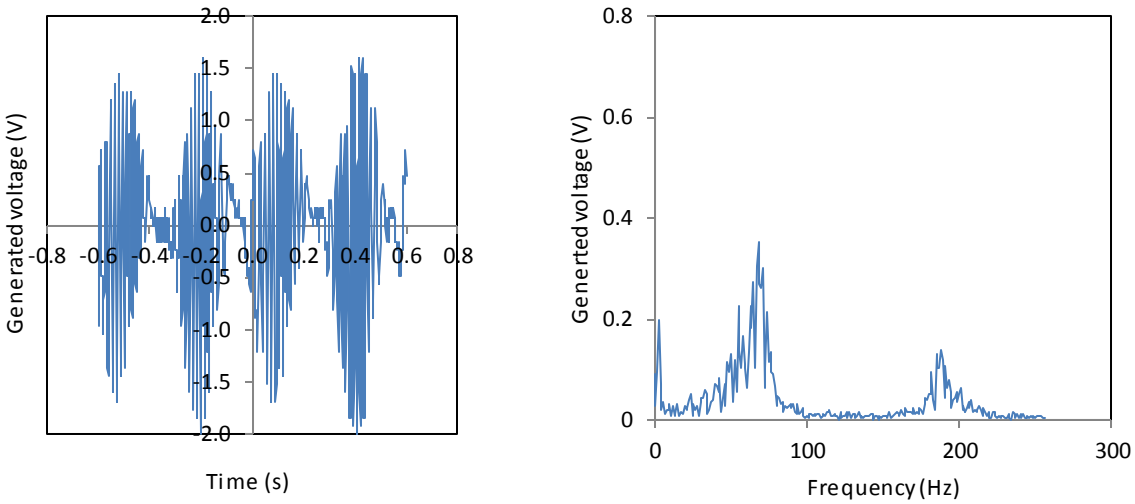

Figure 27 Voltage generation at 3 mm gap

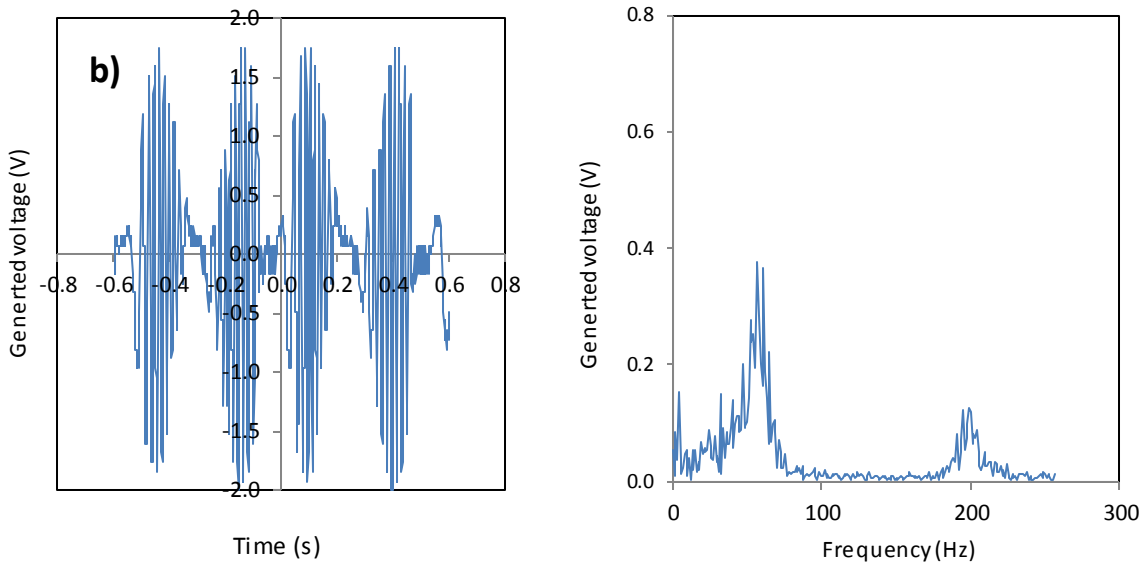

Figure 28 Voltage generation at 2 mm gap

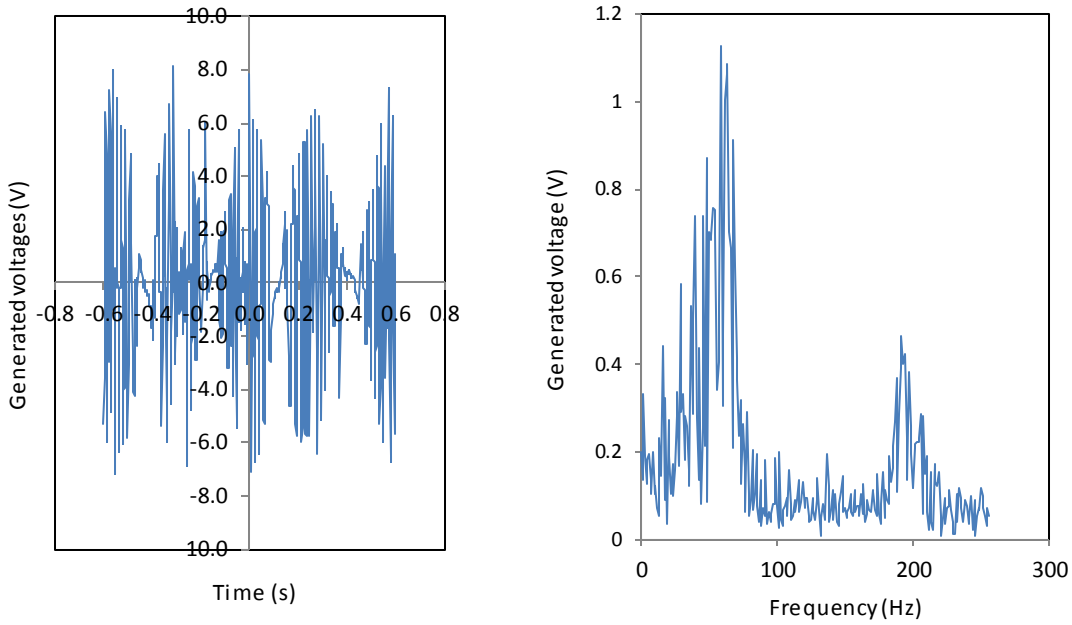

Figure 29 Voltage generation at 1 mm gap

4.3.2 Rotating type

The rotating type was more reliable to conduct electricity generation at 1 mm gap. This is because the spacer attached along the circle to maintain the constant gap during rotation. The rate could be varied from a very low to fast rotation using a drill motor that facilitates acceleration and keeps the fast rotation. Due to the controlled high-speed rotation, the voltage generation was much higher than the sliding type. Another factor affecting the voltage is a considerable number of teeth of the comb-shaped electrode for the rotating type that was larger than that of the sliding type mentioned in previous subsections.

As expected, as the rotation rate increased, the voltages generation also increased. The highest voltage achieved was 1.830 V at a rotating speed of 178 rpm. However this voltage is still not enough to light common LED lamps which usually require at least 3 V in input voltage. Thus, the electronic circuit was found to be necessary to improve the electrostatic vibration energy harvester that will be explained in the next subsection.

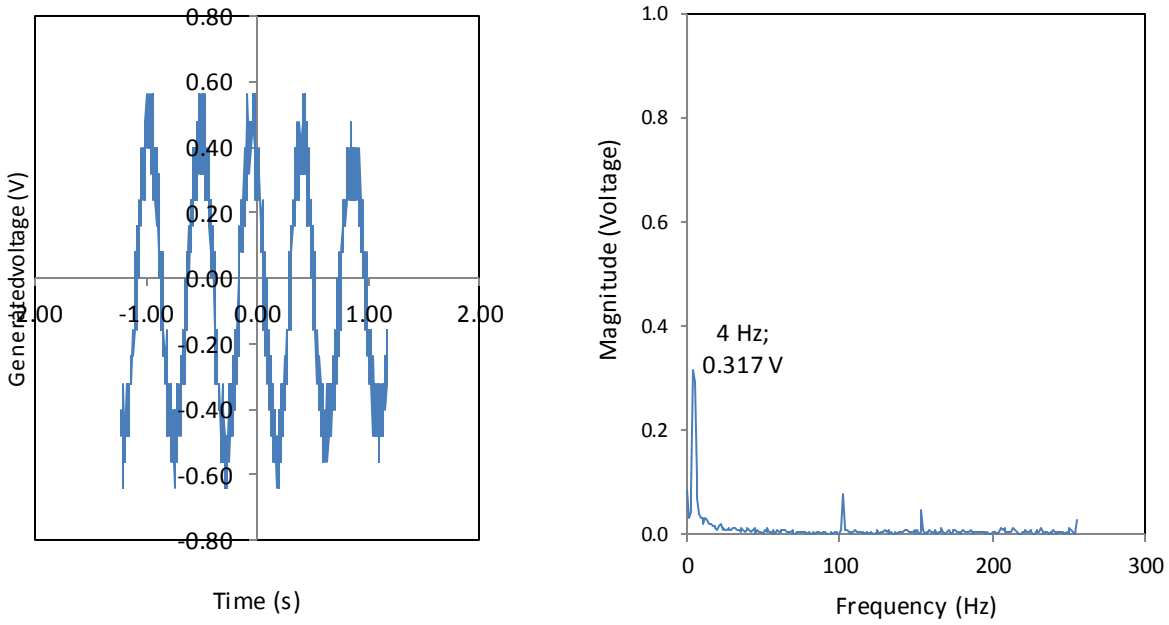

Figure 30 Voltage generation at 10 rpm

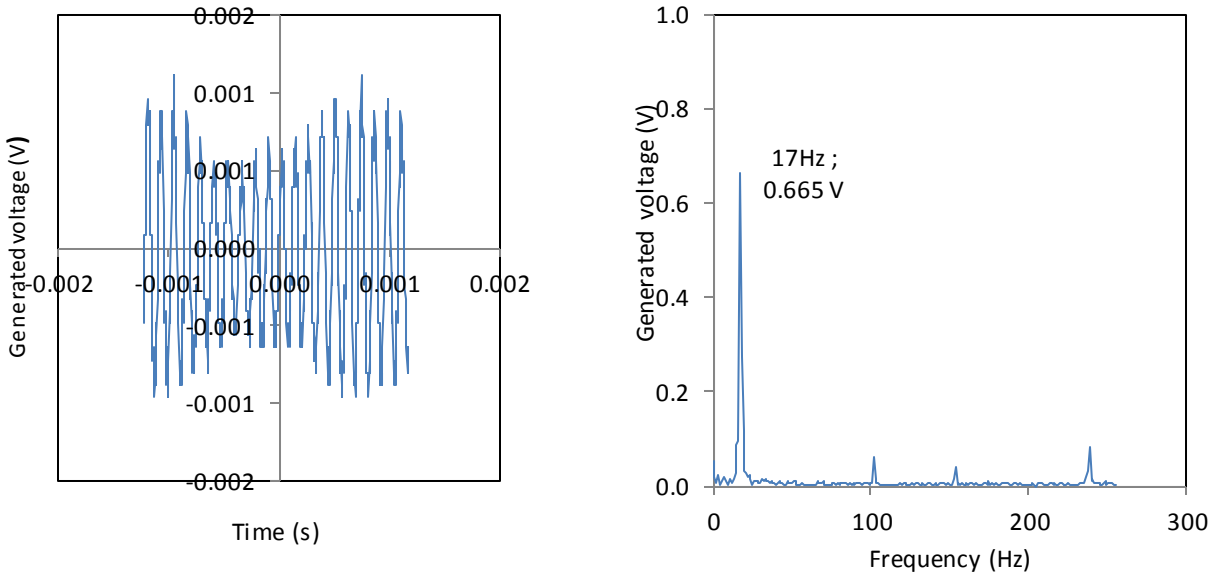

Figure 31 Voltage generation at 26 rpm

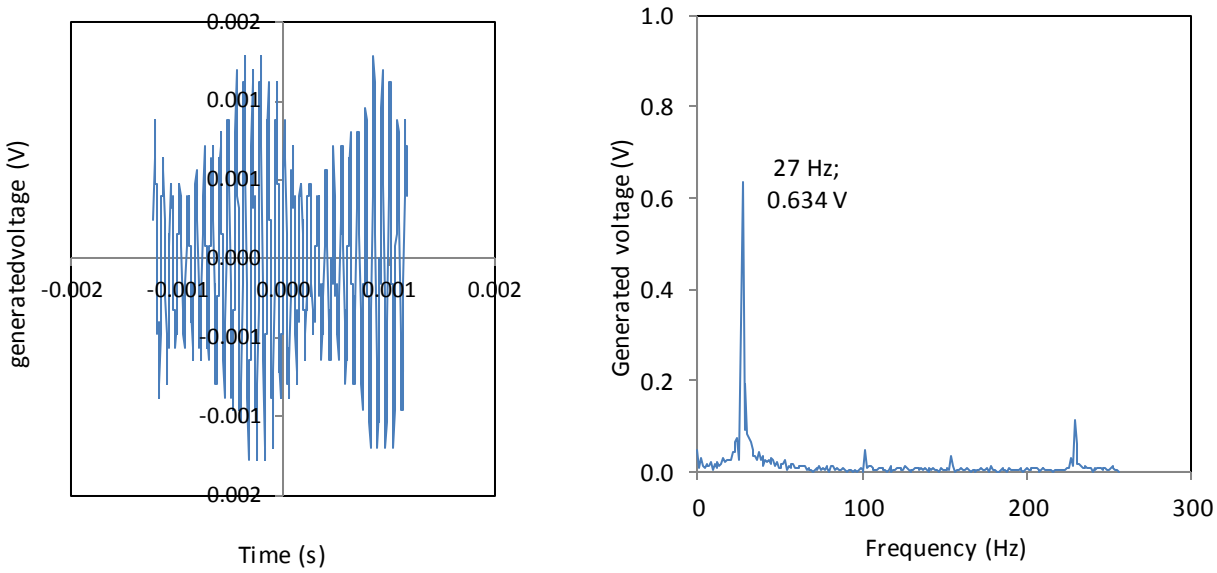

Figure 32 Voltage generation at 46 rpm

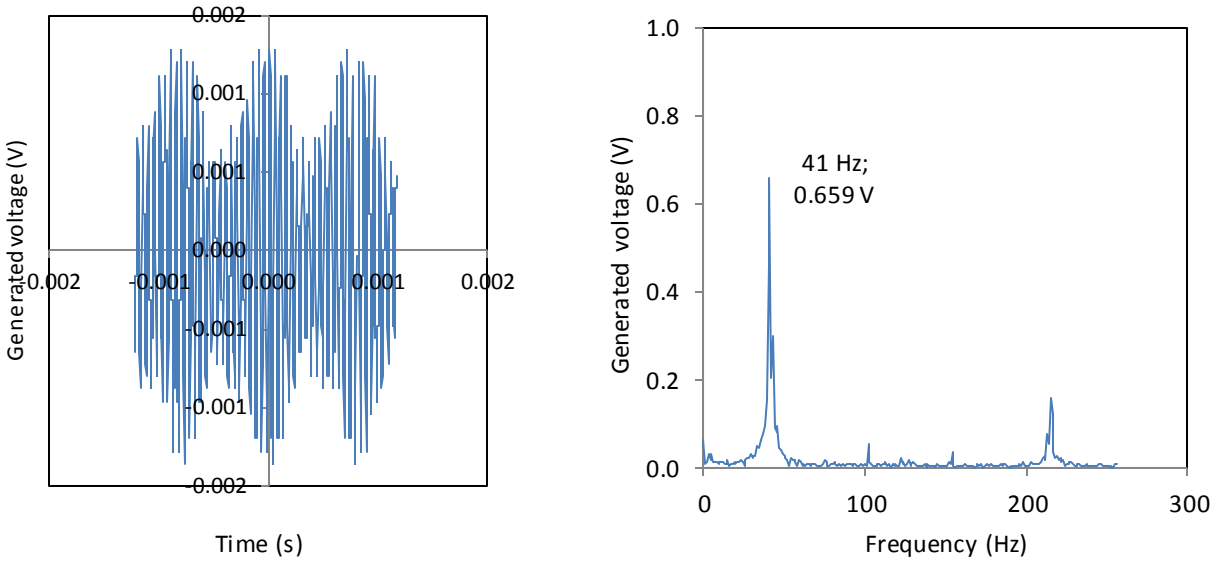

Figure 33 Voltage generation at 70 rpm

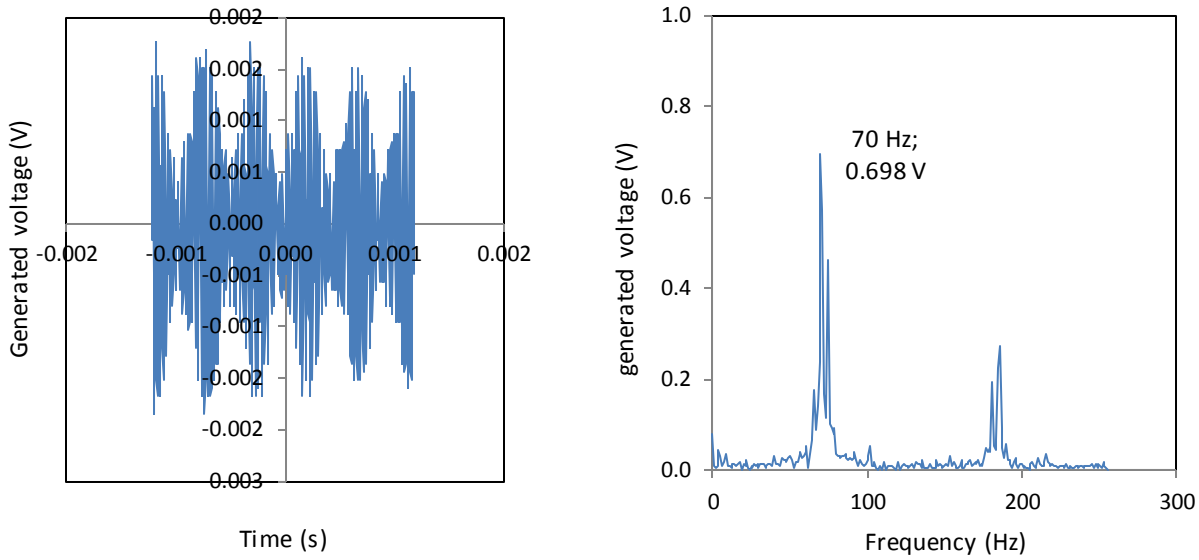

Figure 34 Voltage generation at 125 rpm

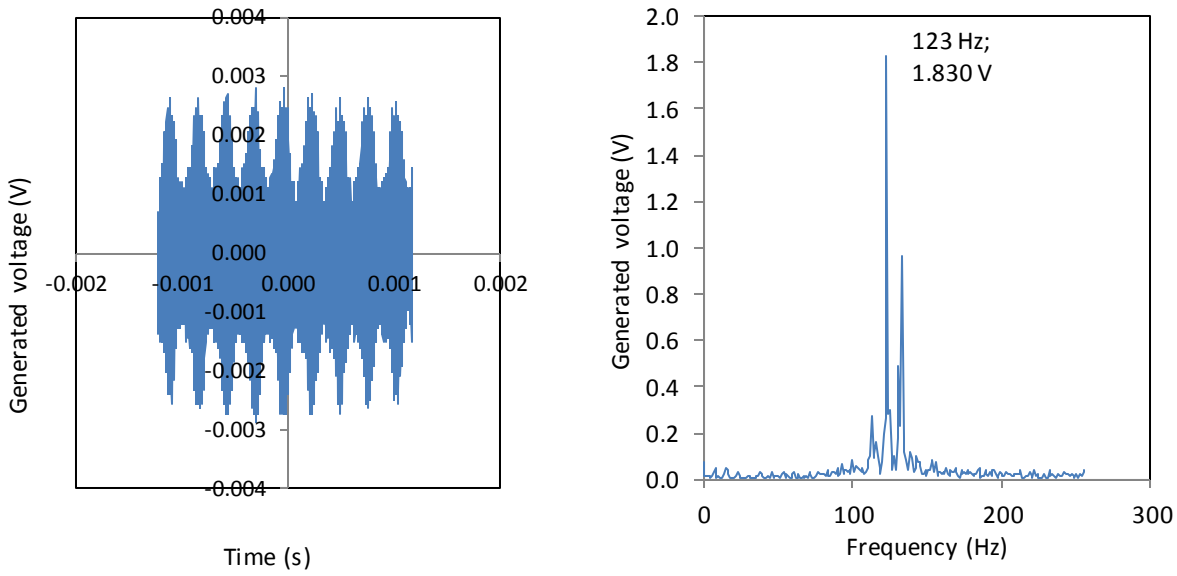

Figure 35 Voltage generation at 178 rpm

4.4 Conclusion

For the sliding type, as the frequency increase as well as the gap decreases, the voltage generation increased significantly. The rotating type provides higher and smoother voltage generation due to multiplication of vibration movements. This TriboEG momentarily generated its highest voltage amplitude of 8.2 V with manual strokes in the sliding in-plane direction of the paperboard vibration. These results suggest that it is possible to harvest vibration energy from both longitudinal and transverse waves in environmental sound sources such as noise and the human voice. The practical displacement of paper surfaces due to sonic wave propagation is small even for transverse waves; however, microelectrodes and microelectrets printed on two sheets of paper with smoothly finished surfaces at a high resolution could be an electric power source for microelectronics in the future.

CHAPTER V

5 OVERALL CONCLUSION

Emerging new technology such nanogenerator can harvest energy from waste source i.e. vibration, heat, and light. Mechanical sources even tough do not provide high power density but quite enough to light some LED lamps in terms of the vibration energy harvesting (VEH) application. From several energy conversion mechanisms such as piezoelectric, electromagnetic, and electrostatic systems, we chose an electret transducer for electrostatic system to achieve low weight and compatible to paper structure. Electret which consist in condenser microphone model was introduced to this out-of plane technique. The dynamic stage of microphone is a magnetic omnidirectional constructed with light diaphragm, the same way as small loudspeaker. This diaphragm is coupled to a suspended coil in strong magnetic field. When the diaphragm and coil move together in sympathy with the sound waves, thus an electric current is generated. This type has a merit of high enough flexibility in mechanical design using paper and PTFE sheets. Paper is neutral in terms of electrical charge, and a PTFE sheet acts as an electret. Electret is a dielectric material with permanent negative electric field that is achieved by rubbing it with another paper and corona treatment.

Paper, formed as a cellulosic fibers network, has been recognized as an eco-friendly and sustainable material. It has some advantages such as light weight, flexibility, and low cost. Paper tends to have neutral charge on its surface and has a large charge differences with PTFE. Thus electrostatic induction is suitable for VEH. Thus it has to fulfill the concept of electrostatic vibration energy harvesting system: 1) has two electrodes called “guard and collector” electrodes, or “moving and static” electrodes, or “dynamic and static” electrodes, etc. that has potential differences to obtain charge movement, 2) has a generator called “electret”, that is a

dielectric material that has a quasi-permanent electric charge or dipole polarization. Usually made from polymer insulator such as PTFE, 3) has a proof or mobile mass that can be provided by paper in this research and 4) has a spring system to generate a resonance phenomenon that can be provide by flexibility of paper.

This research scheme studied on vibration source, convert the vibration by electrostatic phenomenon, and its application in power generation. The vibration energy was evaluated using an electret microphone condenser with nonwoven cloth for protection from dust and airflow noise. The various types of paper were tested as substitutes of the nonwoven cloth to evaluate the rule of paper's type in vibration energy transfer.

Paper-based electrostatic power generators (TriboEG) are being developed to supply low-power consumption and electrostatically induced electric power conversion from environmental noises in the same device. The purposes of this research are 1) to clarify the relationship between vibration damping and the mechanical properties of paper in order to realize efficient power generation by preventing vibration damping; 2) to convert sonic waves such as environmental noise, voice, and sound to electric energy as the final purpose.

This study reports the trial simulation data for future application of paper vibration due to environmental noise, voice, and sound as an energy source with voltage obtained from a prototype paperboard TriboEG. In this system, the weight and elasticity of paper in itself function as a proof mass and spring, respectively. During vibration, the paper keeps energy and it immediately transfers to electricity via electrostatic induction.

Vibration damping was evaluated by measuring the sound power level of acoustic waves traveling through various types of paper in the thickness direction. The resulting sound power level was not related to the in-plane specific Young's modulus of paper. However, it decreased with increasing paper thickness because longitudinal waves being transmitted through paper lose

vibration energy along the traveling distance because of compression in the thickness direction. Furthermore, laboratory sheets were subjected to concurrent measurements of the sound power level and in-plane Young's modulus with an ultrasonic tester. The in-plane specific Young's modulus was confirmed to be a key parameter affecting the sound power level because the propagating surface waves travel in the in-plane direction and they were transverse waves with in-plane compression. Regarding papermaking materials, there was no difference in vibration damping tendency between hardwood and softwood bleached kraft pulps.

Electric energy could be generated using a simple TriboEG with paperboard as a vibration transmission medium and PTFE as an electret. Based on the dual wave nature of sound in which longitudinal and transverse waves propagate in a solid material, two types of TriboEGs are established in : 1) the out-of-plane without any comb-shaped pattern which is effective for realizing a high surface potential. and 2) in-plane modes with comb-shape pattern represented by sliding and rotating types. These TriboEG systems successfully generated their highest voltage amplitude of 3.5 V at a forced vibration frequency of 46 Hz and highest output power 11.8 μW at 2 MOhm load resistance and 39 Hz both in the out-of-plane direction of the paperboard vibration. The other type of TriboEG momentarily generated its highest voltage amplitude of 8.2 V and 8.684 nW at low frequency of 3 – 4 Hz with manual strokes in the in-plane direction of the paperboard vibration. These results suggest that it is possible to harvest vibration energy from both longitudinal and transverse waves in environmental sound sources such as noise and the human voice. The practical displacement of paper surfaces due to sonic wave propagation is small even for transverse waves; however, microelectrodes and microelectrets printed on two sheets of paper with smoothly finished surfaces at a high resolution could be an electric power source for microelectronics in the future.

REFERENCES

Kasuga Denki, Inc. (2012). Retrieved 11 11, 2015, from www.ekasuga.co.jp: www.ekasuga.co.jp/en/product/185/000232.shtml

Alphalab Inc. (2012, 2 16). *The Triboelectric Series*. Retrieved 4 2, 2013, from Alphalab Inc.: https://www.trifield.com/content/tribo-electric-series/

Arakawa, Y., Suzuki, Y., & Kasagi, N. (2004). Micro seismic power generator using electret polymer film. *Proceedings of the 4th International Workshop on Micro and Nanotechnology for Power Generation and Energy Conversion Applications* (pp. 188-190). Kyoto: IEEE.

Bae, J., Lee, J., Kim, S. M., Ha, J., Lee, B. S., Park, Y. J., et al. (2014). Flutter-driven triboelectrification for harvesting wind energy. *Nature Communications, 5*, p. 4929.

Baum, G. A., Brennan, D. C., & Haberger, C. C. (1981). Orthotropic elastic constants of paper. *TAPPI Journal*, 97-101.

Beeby, S., Tudor, M., & White, N. (2006). Energy harvesting vibration sources for mycrosystems applications. *Measurement Science Technology, 17*, 175-195.

Bhatnagar, V., & Owende, P. (2015). Energy harvesting for assistive and mobile applications. *Energy Science & Engineering*, 153-173.

Boisseau, S., Despesse, G., & Seddik, B. A. (2012). Electrostatic conversion for vibration energy harvesting. In *Small-Scale Energy Harvesting* (pp. 1-39). Intech.

Boisseau, S., Duret, A. B., Chaillout, J. J., & Despesse, G. (2012). New DRIE-patterned electrets for vibration energy harvesting. *2nd European Energy Conference*, (pp. 1-8). Maastricht.

Boland, J., Chao, Y., Suzuki, Y., & Tai, Y. (2003). Micro electret power generator. *The 16th Annual International Conference* (pp. 538-541). Kyoto: IEEE.

Briscoe, J., Jalali, N., Wooliams, P., Stewart, M., Weaver, P. M., Cain, M., et al. (2013). Measurement techniques for piezoelectric nanogenerators. *Energy and Environmental Science*.

Challa, V. R., Prasad, M. G., Shi, Y., & Fisher, F. T. (2008). A vibration energy harvesting device with bidirectional resonance frequency tunability. *Smart Material Structure, 17*, 1-10.

Chen, B. M. (2008). *Courses: Ch 3 Diodes, Rectifiers, and Power Supplies.* Retrieved July 03, 2015, from National University of Singapore web site: http://uav.ece.nus.edu.sg/~bmchen/courses/EG1108_Rectifiers.pdf

Eccardt, P., Niederer, K., Scheiter, T., & Hierold, C. (1996). Surface micromachined ultrasound transducers in CMOS technology. *Proc. IEEE Ultrasoound Symp.*, (pp. 959-962). San Antonio, TX.

Genda, T., Tanaka, S., & Esashi, M. (2004). High power electret motor and generator on shrouded turbine. *PowerMEMS 2004* (pp. 183-1862004). Kyoto: IEEE.

Guo, H., Chen, J., Leng, Q., Xi, Y., Wang, M., He, X., et al. (2015). Spriral interdigital-electrode-based multifunctional device: Dual-functional triboelectric generator and dual-functional self-powered sensor. *Nano Energy*, 626-635.

Haberger, C. C., Mann, R. W., & Baum, G. A. (1979). Ultrasonic plate waves in paper. *Ultrasonics, 17*(2), 57-62.

Hagiopol, C., & Johnston, W. J. (2011). Chemistry of modern papermaking. NW: CRC Press.

Honzumi, M., Ueno, A., Hagiwara, K., & Suzuki, Y. (2010). Soft-X-Ray-charged vertical electrets and its application to electrostatic transducers. *MEMS 23rd International Conference* (pp. 635-638). Wangchai, Hong Kong: IEEE.

Hsu, T. Y., Hsich, W. H., Tai, Y. C., & Furatani, K. A. (1996, June 3-6). Thin film electret technology for microphone applications. *Solid-state Sensor and Actuator Workshop* , (pp. 235-239). Hilton Head Island, SC.

Karagozler, M. E., Poupyrev, I., Fedder, K. G., & Suzuki, Y. (2013). Paper generators: harvesting energy from touching, rubbing & sliding. *The 26th Annual ACM Symposium on User Interface Software & Technology* (pp. 23-30). New York, USA: Association for Computing Machinery.

Karki, J. (2000). *Effect of parasitic ccapacitance in op amp circuits.* Texas: Texas Instruments.

Khoury, M., Tourtoller, G. Y., & Schroder, A. (1999). Contactless measurement of the elastic Young's modulus of paper by an ultrasonic technique. *Ultrasonics, 37*, 133-139.

Ladabaum, I., Jin, X., Hyongsok, T., Atalar, A., & Khuri-Yakub, B. T. (1998). Surface micro machined capacitive ultrasonic transducers. *IEEE, 45*, 678-690.

Lahti, J., & Tuominen, M. (2007). The effects of corona and flame treatmnet: Part 1. PE-LD coated packaging board. *11th European Tappi PLACE Conference*, (pp. 1-15). Athens, Greek.

Lamb, H. (1910). *The dynamical theory of sound.* (E. Arnold, Ed.) London.

Lee, Y. C., & Chiu, Y. (2011). Low cost out-of-plane vibrational electret energy harvester. *The 11th International Workshop on Micro and Nanotechnology for Power Generation and Energy Conversion Applications* (pp. 1-4). Seoul: PowerMEMS.

Liang, Q., Zhanga, Z., Yan, X., Gu, Y., Zhao, Y., Zhang, G., et al. (2015). Functional triboEG as self-powered vibration sensor with contact mode and non-contact mode. *Nano Energy*, 209-216.

Liu, C., & Bard, A. J. (2008). Electrostatic electrochemistry at insulators. *Nature Material, 7*, 505-509.

Matsumoto, K., Saruwatari, K., & Suzuki, Y. (2012). Prototyping battery-less wireless sensor node using electret-based kinetic energy harvesting. *Transactions on Electronics, Information and Systems, 132*, 344-349.

Miranda, J. M. (2004). *Electrostatic vibration-to-electric energy conversion.* Massachusetts: Massachussets Institute of Technology.

Naruse, Y., Matsubara, N., Mabuchi, K., Izumi, M., & Honma, K. (2008). Electrostatic micro power generator from low frequency vibration such as human motion. *Proceedings of PowerMEMS*, (pp. 19-22). Sendai.

Paajanen, M., Wegener, M., & Gerhard-Multhaupt, R. (2001). Understanding the role of the gas in the voids during corona charging of cellular electret films - a way to enhance their piezoelectricity. *J. Phys.D: Appl. Phys., 34*, 2482-2488.

Paradiso, J. A., & Statner, T. (2005). Energy scavenging for mobile and wireless electronics. *Pervasive Computing*, 18-27.

Patrick, D. R., & Fardo, S. W. (2008). *Electricity and Electronics Fundamental.* The Fairmont Press, Inc.

Ross, R. J., Kan, J., Wang, X., Blakenburg, J., Stockhausen, J. I., & Pellerin, R. F. (2012). *Wood and wood-based materials as sensors -A review of the piezoelectric effect in wood.*

Saad, A., Mescheder, U., Muller, B., & Nimo, A. (2010). High efficient, low cost electret charging set-up for MEMS based energy harvesting systems. *The 10th Intl. Workshop on Micro & Nanotechnology for Power Generations & Energy Conversion Applications* (pp. 61-64). Leuven, Belgium: PowerMEMS.

Sakane, Y., Suzuki, Y., & Kasagi, N. (2008). The development of high-performance perfluorinated polymer electret and its application to micro power generation. *Journal of Micromechanics and Microengineering, 18*, 1-6.

Sato, J., Hutchings, I., & Woodhouse, J. (2008). Determining of the dynamic elastic properties of paper and paperboard from the low frequency vibration modes of rectangular plates. *Appita Journal, 4*, 219-296.

Schlecther, J. (2006). *Visualization of vibrations of loudspeaker membranes.* Dresden: Technical University Dresden.

Sessler, G. M., & West, J. E. (1962). Self-biased condenser microphone with high capacitance. *Journal of Acoustic Society America, 34*(11), 1787-1788.

Shearwood, C., & Yates, R. B. (1997). Development of an electromagnetic micro-generator. *Electronics Letter*, pp. 1883-1884.

Takahashi, T., Suzuki, M., Nishida, T., Yoshikawa, Y., & Aoyagi, S. (2012). Milliwatt order vertical vibratory energy harvesting using electret and ferroelectric -discharge does not occur with small gap and only one wiring is required. *MEMS IEEE 25th International Conference*, (pp. 1265-1268). Paris.

Tao, K., Lye, S. W., Miao, J., & Hu, X. (2015). Design and implementation of an out-of-plane electrostatic vibration energy harvester with dual-charged electret plates. *Microelectronic Engineering, 135*, 32-37.

Tsai, P. P., Schreuder-Gibson, H., & Gibson, P. (2002). Different electrostatic methods for making electret filters. *Journal of Electrostatics, 54*(3), 333-341.

Tsutsumino, T., Suzuki, Y., & Kasagi, N. (2007). Electromechanical modeling of micro electret generator for energy harvesting. *Proceedings of the 14th International Conference of Solid-State Sensors, Actuators and Microsystems*, (pp. 863-866). Lyon.

Tsutsumino, T., Suzuki, Y., Kasagi, N., Kashiwagi, K., & Morizawa, Y. (2006). *Proceedings of the 23rd Sensor Symposium*, (pp. 521-524). Takamatsu.

Tucker, B. J. (2001). *Ultrasonic plate waves in wood-based composite panels.* Washington D.C.: Washington State University.

Wang, L., & Yuan, F. (2007). Energy harvesting by magnetostrictive materials for powering wireless sensors in SHM. *Smart Structures and Materials*, 1-11.

William, C. B., & Yates, R. B. (1996). Analysis of micro-electric generator for microsystem. *Sensors & Actuators A: Physical*, 8-11.

Yang, P. K., Lin, Z. H., Pradel, K. C., Lin, L., Li, X., Wen, X., et al. (2015). Paper-based origami triboelectric nanogenerator and self-powered pressure sensors. *ACS Nano, 9*(1), 901-907.

APPENDIX

DETERMINATION OF ELECTRIC POWER OF PAPER-BASED GENERATOR

I. A. Power factor correction

To confirm the feasibility of paper-based generator, the electronic system should be studied. In this chapter, several electronic circuits were assembled to check the power generation at certain levels. "Power" definitions are known as three equations as follows (Patrick & Fardo, 2008):

the power that is used to do the work on the load is called real power (P)

$$P = V_{rms}\, I_{rms} \cos \Theta \qquad (1)$$

The power that is wasted and not used to do work on the load is called reactive power (Q)

$$Q = V_{rms}\, I_{rms} \sin \Theta \qquad (2)$$

The power that is supplied to the circuit is called apparent power (S)

$$S = V_{rms}\, I_{rms} \qquad (3),$$

where,

V_{rms} is a voltage root mean square, $V_{peak}/\sqrt{2}$ in volt (V)

I_{rms} is a current root mean square, $I_{peak}/\sqrt{2}$ in ampere (A)

Θ is the apparent power phase angle or impedance phase angle.

In AC circuits, the power factor is the ratio of the real power to the apparent power. The power factor value ranges from 0 to 1. Usually, in inductive load, all the power is reactive power with

no real power, thus the power factor is 0. Meanwhile, in resistive load, all the power is real power with no reactive power, thus the power factor is 1.

To calculate the power factor, we use this equation:

$PF = P / |S|$,

where,

PF is the power factor;

P is the real power in watt (W).

$|S|$ is the apparent power - the magnitude of the complex power in volt·amp (VA)

The power factor PF is equal to the absolute value of the cosine of the apparent power phase angle Θ for sinusoidal current.

$$PF = |\cos \Theta|$$

PF is the power factor.

Adjustment of an electrical circuit should be made in order to improve the power factor to nearly 1. It would reduce the reactive power in the circuit. This would also reduce power lines losses. Capacitors are usually added to the load circuit.

The apparent power $|S|$ in volt-amp (*VA)* is equal to the voltage V in volt (V) times the current I in amp (A):

$$|S_{(VA)}| = V_{(V)} \times I_{(A)} \qquad (4)$$

As in Pythagorean theorem, the reactive power Q in volt-amps reactive (VAR) is equal to a square root of the square of the apparent power |S| in volt-ampere (VA) minus the square of the real power P in watt:

$$Q_{(VAR)} = \sqrt{(|S_{(VA)}|^2 - P_{(W)}^2)} \qquad (5)$$

The reactive power is also expressed as follow:

$$Q_{(VAR)} = V_{(V)}^2 / X_C = V_{(V)}^2 / (1 / (2\pi f_{(Hz)} \cdot C_{(F)})) = 2\pi f_{(Hz)} \cdot C_{(F)} \cdot V_{(V)}^2 \qquad (6)$$

This equation leads to how much capacitor in farad (F) that should be added to the circuit in parallel. The equation is as follow:

$$C_{(F)} = Q_{(VAR)} / (2\pi f_{(Hz)} \cdot V_{(V)}^2) \qquad (7)$$

I. B. Circuit set-up

Electronics systems were fabricated using several components such as resistors, capacitors, bridge rectifiers, alligator clips, breadboard, oscilloscope, and impedance analyzer (Hioki, Inc IM3590). Several circuits are shown in Figure A.1 and Figure A.2 as follow:

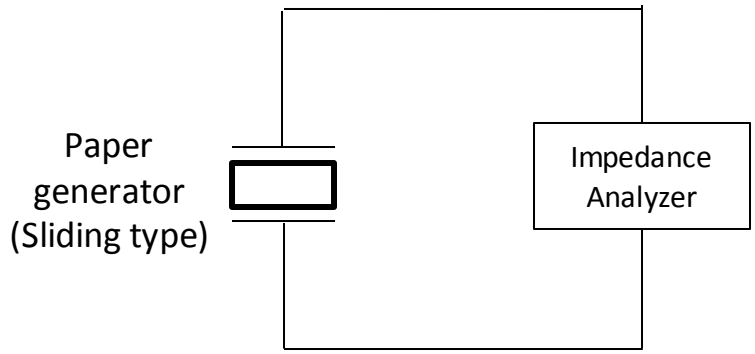

Figure A. 36. Paper generator connected directly to impedance analyzer

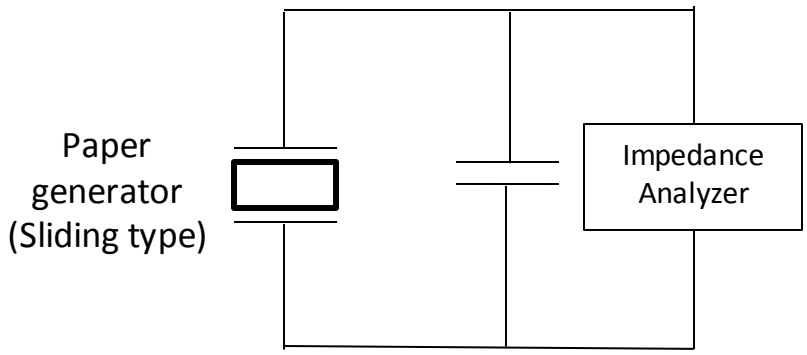

Figure A. 37. Paper generator connected to impedance analyzer parallel to capacitor

In Figure A.1, the impedance analyzer was set to the condition at a minimum voltage CV = 0.0005V, minimum current CC = 0.01 mA, the frequency of the impedance analyzer 10 Hz, and internal trigger to provide more sensitive measurements.

In paper-based generator, as electret in the moving part moves relatively to the fixed part, capacitance changes should be taken into account (Boisseau, Despesse, & Seddik, Electrostatic conversion for vibration energy harvesting, 2012); (Karki, J, 2000); (Miranda, 2004). Mostly in electronic circuits, parasitic capacitance is undesirable. Unlike common types, due to its natural dielectricity, the paper-based generator shows positive behavior which is practically not suitable to be called "parasitic capacitances", although it is only in picofarad. Thus, the additional external capacitor will be also assembled parallel with the paper-based generator. Figures A.2 and A.3 show two circuits to help understand the behavior of power generation in two methods as the meaning of different function to each component.

In Figure A.3, a bridge rectifier of 0.8V and a maximum input 800 V was added to realize the practical application of electrostatic vibration energy harvesting. Because the vibration source is a sinusoidal resonance movement which is analogous to an AC source, it is necessary to convert it into DC current (Chen, 2008). The converter component to obtain a full wave is a bridge rectifier. It consists of 4 bridging diodes. Every bridge rectifier has a forward voltage drop, which largely impacts the voltage generation due to a small course of electrostatic movement. Another smaller forward drop in voltage, such as Zenner diode or Schottky diode, should be added.

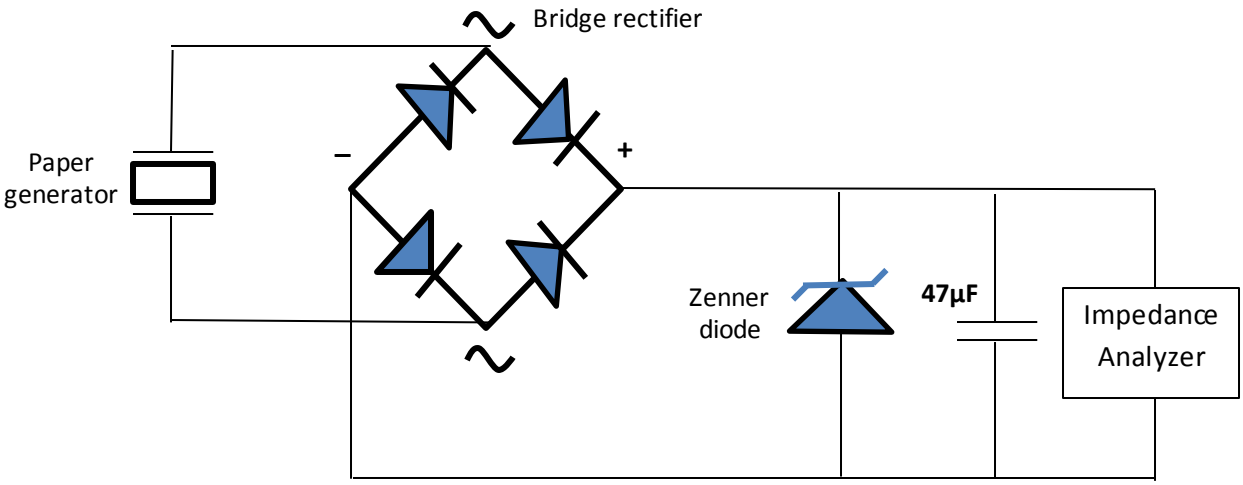

Figure A. 38. Paper-based generator circuit

In Figure A.4, power generation was conducted using several load resistors. The external load resistor is necessary to regulate the electrical current produced by vibration movement.

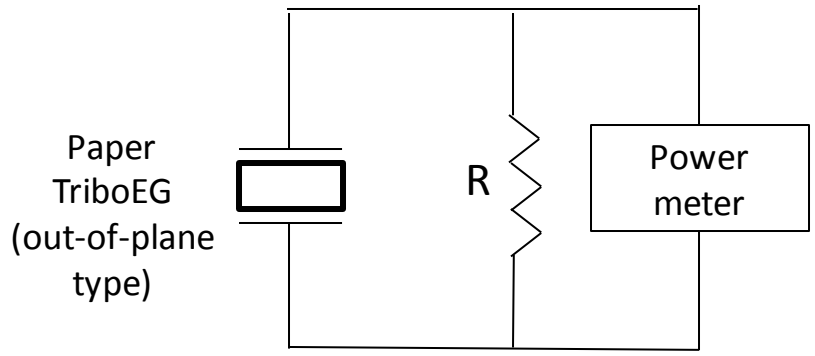

Figure A. 4. Paper generator connected to power meter parallel to load resistor

I. C. Impedance analyzer measurement

The experiment of the circuit represented in Figure A.1 provided data as shown in Table A.1. The result shows a real power of 2.197 nW, apparent power of 2.275 nW, and reactive power of 0.078 nW. Equation (6) was applied to calculate the reactive power from the data measured with the impedance analyzer using 10 Ω reactance (X) that resulted in 0.122 mΩ. These data were then used to calculate capacitor that should be added for power factor correction, i.e., at least 45.31 µF. The oscilloscope was used to confirm the input frequency of a slow manual operation, i.e., 3 – 4 Hz. Table A.2 shows impedance analyzer data after using a 47 µF capacitor for power factor correction.

Table A.1. Observation of paper-based generator connected directly to impedance analyzer

Parameter	Value (unit)
Z (impedance)	350 ± 98 Ω
X (reactance)	10 ± 7 Ω
Θ (impedance angle)	15 ± 9 °
Iac (current AC across the probes)	13 ± 5 μA
Vac (voltage AC across the probes)	3.5 ± 0.2 mV

Table A.2. Observation of paper-based generator function after capacitor correction

Parameter	Value (unit)
Z = impedance	250 ± 43 Ω
X = Reactance	250 ± 26 Ω
Θ = impedance angle	-40 ± -5 °
Iac = current AC across the probes	19.5 ± 3.1 µA
Vac = voltage AC across the probes	4.5 ± 0.2 mV

The power was calculated by using equation $P=V^2/R$ as follow:

$$P(t) = V(t) \cdot I(t) = V_0 \sin \omega t \cdot \frac{V_0}{Z \cos\theta} \sin \omega t = \frac{V_0^{\,2}}{Z \cos\theta} \sin^2 \omega t \tag{8}$$

$$P = \frac{1}{T}\int_0^T P(t)dt = \frac{1}{T}\int_0^T P(t)dt = \frac{V_0^{\,2}}{ZT \cos\theta}\int_0^T \sin^2 \omega t dt = \frac{V_0^{\,2}}{2ZT \cos\theta}\int_0^T (1-\cos 2\omega t)dt \tag{9}$$

Where $T=2\pi/\omega$ therefore,

$$P = \frac{V_0^{\,2}}{2Z \cos\theta} \tag{10}$$

P= (4.5 x 10^{-3})^2/(2 x 250 x cos (-40)) = 5.287 µW

This power is much higher than that extracted from Table A.1., i.e., 1.777 nW (P= (3.5 x 10^{-3})^2/(2 x 350 x cos (10°)).

Table A.3 shows the observation of paper generator using bridge rectification in order to get any DC current. Every device, even connected to AC as a power source, necessarily requires DC converted from the AC in order to work it, for example, to light an LED lamp.

Table A.3. Observation of paper generator using rectification

Parameter	Value (unit)
Z = impedance	104 Ω
X = Reactance	-82.7 mΩ
Θ = impedance angle	–59 °
Cp= parallel capacitance	47 μF
Iac = current AC across the probes	31.6 μA
Vac = voltage AC across the probes	3.05 mV

Although the generated voltages were not high enough due to the design and dimension limitations of a bridge rectifier, the output voltage remained stable, which means that the rectification from AC to DC was confirmed. As every diode rectifier has a forward voltage drop, it was approximately 0.5 V in this experiment. However, the whole data in Table A.3 shows such an effect that the rectification lowered the impedance of the system, thus resulted in much higher power, i.e., 8.684 nW ($P = (3.05 \times 10^{-3})^2/(2 \times 104 \times \cos(-59°))$).

Figure A.5 shows the measured output power densities of out-of-plane TriboEG with a maximum value of 11.8 μW at a load of 2 MΩ. Although the μW order power seems fairly small, it is high enough to light an LED at instantaneous power generation. A maximum value was attained when the load resistance is equal to the internal resistance of the TriboEG circuit as is usually large.

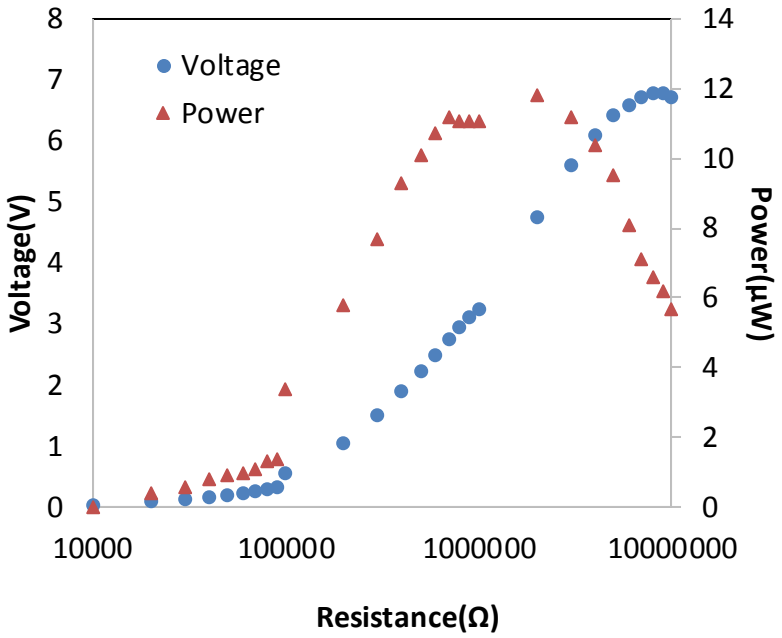

Figure A. 5. Voltage and power generation with load resistance

ACKNOWLEDGMENT

I would like to express my deepest gratitude to my supervisor, Professor Toshiharu Enomae, whose expertise, persistence, understanding, kindness and patience, added considerably to my graduate experience. I appreciate his vast knowledge and skill in many areas such vision, ethics, and interaction with lab members, and his assistance in writing reports. I have been amazingly fortunate to have an advisor who gave me the freedom to explore on my own, and at the same time the guidance to recover when my steps faltered. His support helped me overcome many crisis situations and finish this dissertation.

I would like also to use this opportunity to express my gratitude to Professor Hiroshi Ohi, Associate Professor Akiko Nakagawa-Izumi, and Associate Professor Eiichi Obataya who kindly supported throughout the research experiments of my PhD course.

A special thanks to Ms. Yohko Naruse, Panasonic Corporation, Japan for valuable comments about the TriboEG design, Professor Yuji Suzuki, the University of Tokyo, Japan, for the corona discharge treatment and valuable suggestions, Dr. Ken-ichi Nomura, National Institute of Advanced Industrial Science and Technology, Japan, Mr. Daisuke Shigeta, Hioki E.E. Corp., Japan for valuable discussion on the measurement of the power, and Masato Morii for his technical support during power generation experiment in my hard time.

Thank you for the great support from Mr Ngakan Timur Antara, Mrs Nina Elyani, Mr Posma R. Panggabean, and Mr Andoyo Sugiharto from Center of Pulp and Paper, Ministry of Industry, Indonesia that provided me with direction, technical support and became more of a mentor and friend.

I must also acknowledge the electrical-related engineers Toni Rachmanto, Muhammad Restu, Nadine Nandanari and her husband Araf Pratamanaim for their suggestions throughout my graduate program. Thanks also go out to Sachnaz Desta Oktarina who provided me with statistical advice. I would also like to thank my friends in Biomaterial and Eco-friendly Paper Device Lab, Dr. Tunchira Bunyapiphat, Dr. Tithimannan Srimongkon, Yinchao Xu, Hu Donghao, Siti Dian Mardiyani, Abdul Halim, Yukiko Mochizuki and Bioresources lab members for our exchanges of knowledge, skills, and venting of frustration during my graduate program, which helped enrich the experience, and to the office staff, especially to Mrs Shigure Shimazaki, for all the instances in which their assistance helped me along the way.

I would also like to thank my family for the support they provided me through my entire life and in particular, I must acknowledge my husband Ewan Kurniawan without whose love and understanding I would not have finished this thesis.

I recognize that this research would not have been possible without the financial assistance of Scholarship fund from Ministry of Education, Culture, Sport, Science & Technology (MEXT) Japan, University of Tsukuba (2013 Grant-in-Aid for Scientific Research Type B) and Japanese Society of Printing Science and Technology (2015 Printing Technology Research Fund).